ABSTRACT

KOEHLER, CYNTHIA LAUREN. Engineering a DNA Origami Tool for Multiscale Investigation of Cell Signaling. (Under the direction of Dr. Thomas H. LaBean).

Nanoscale patterning of surfaces is a high potential application of DNA nanotechnology. The use of DNA origami to achieve this goal in an *in vivo* setting has direct applications in the exploration and control of cell signaling processes. Cells receive signals both chemically and mechanically, the latter through the process of mechanotransduction, which converts external mechanical forces exerted on the cell to internal chemical cascades. Both processes direct many cellular responses, such as attachment and migration, and it is apparent that there is significant interplay between these two signaling regimes. However, investigating the dynamics between the processes is far from straightforward, in large part because they occur at different length scales: nanoscale for chemical signaling, and up to the microscale for mechanotransduction. This project aims to address the problem of investigating cell signaling across length scales and between chemical and mechanical input through a multiscale tool comprised of DNA origami, a chimeric molecule with peptide nucleic acid (PNA) and peptide segments, and films with tunable viscoelastic properties constructed from colloidal microgels. Understanding cell signaling opens the opportunity to direct it, which in turn has great potential in medical fields, particularly in the realm of wound healing.

Transforming growth factor beta (TGF-β) is a cytokine that exhibits multiple effects on cellular functions, including the control of cell growth, differentiation, and proliferation. TGF-β is essential to the progression of wound healing, as it is involved in nearly every step of the cascade, and the timing of its signal input to cells is critical – improper TGF-β signaling can result in either chronic wounds or excessive scarring. TGF-β receptors are thought to

oligomerize, first dimerizing and then forming higher order clusters, following binding of TGF-β. In the absence of the growth factor, monomeric receptors are distributed randomly across the surface of the cell. Understanding the connection between TGF- β receptor clustering and activation of the receptor's phosphorylation domain in the cytoplasm is an important basic science and potential medical technology issue. Previous studies have shown that cells can be sensitized to the presence of TGF-β (i.e. made more responsive to a lower concentration of the chemical signal) by pre-clustering their TGF-β receptors via presentation of a peptide patterned on DNA origami.

DNA origami are ideal for this application as they can be functionalized at discrete sites with molecular (i.e. low nanometer scale) precision. Strand modifications at chosen sites allow for hybridization with the complementary sequence of the custom PNA-peptide. The PNA-peptide chosen for this project binds non-agonistically to TGF-β receptors, which allows for pre-clustering of the receptors without interfering with the TGF-β binding sites. Furthermore, separate strand modifications on the origami structure allow for covalent conjugation between aminated oligonucleotide extensions and acrylated colloidal microgels enabling controlled coupling of origami and microgel films. Tuning the stiffness of the microgels via chemical crosslinking between particles provides the mechanical input to cells that is necessary to explore microscale mechanotransduction in addition to nanoscale chemical signaling, thus completing the multiscale tool.

This project used a combination of atomic force microscopy, various fluorescence methods, and 24 hour live cell assays to characterize this system. The hypothesis anticipated that TGF-β signaling in live cells would increase in the presence of DNA origami and pre-patterned receptors. Initial data exploring this hypothesis is presented here, as well as advances in the

characterization of composite polymer film/DNA origami materials. This and following studies could enable meaningful advances in the development of future wound healing treatments.

Engineering a DNA Origami Tool for Multiscale Investigation of Cell Signaling

by
Cynthia Lauren Koehler

A thesis submitted to the Graduate Faculty of
North Carolina State University
in partial fulfillment of the
requirements for the degree of
Master of Science

Materials Science and Engineering

Raleigh, North Carolina
2021

APPROVED BY:

_____	_____
Dr. Thomas H. LaBean Committee Chair	Dr. Ashley C. Brown
_____	
Dr. C. Reynolds	

DEDICATION

For mom, dad, Brian, and all the wonderful friends I have made along the way

BIOGRAPHY

Cynthia was born and raised in St. Louis, Missouri, and lived the majority of her formative years within walking distance of both the world's largest Amoco sign and Forest Park. Her parents discovered early on that she could be bribed into (mostly) good behavior with gooey butter cake. She started talking ahead of developmental schedule and has never shown any signs of stopping, and learned how to speak a few languages in order to give herself a greater chance of being able to yammer to everyone she meets, not that being incomprehensible has ever stopped her before. She completed her freshman year of college at the College of William and Mary, where she thought that she would major in Linguistics, before deciding to transfer. She worked for a year in the laboratory of Professor Himadri Pakrasi at Washington University in St. Louis, where she began to admit her love of the STEM fields to herself. She transferred to The University of Missouri-Columbia to study engineering, as her mother had always suggested. There, she was fortunate enough to receive funding from the IMSD EXPRESS program to perform undergraduate research in the laboratory of Professor Jason Cooley. She received a Bachelor of Science in Mechanical Engineering with a minor in Mathematics in December of 2015, and joined Professor Thom LaBean's research group at North Carolina State University in 2016 after spending all of her money backpacking around Europe for two months. Cynthia hopes to use everything she has learned to leave every place she goes a little better than how she found it.

ACKNOWLEDGMENTS

I'd like to acknowledge Professor Thom LaBean for giving me the opportunity to conduct research at this level. Without his patience and support, literally none of this would have been possible. I would also like to thank him for giving me the chance to explore teaching in a collegiate environment, and for his magnanimity during the times that I have been flippant and unprofessional.

I'd like to thank my group members, past and present: Dr. Jacob Majikes, my older lab brother who always makes time as a mentor and friend, who I consider myself truly fortunate to know; Dr. Abhichart Krissanaprasit, who teaches me something about how to be a better scientist every time we speak and brings fun with him wherever he goes; Nikolay Frik, who knows the good wine and chocolate; Mahshid Hosseini, who always makes time spent in the lab and the office warm and pleasant; Ming Gao, Wonder Woman, always ready for a friendly conversation and an adventure; and all of the undergraduates who have helped and put up with me along the way.

Someone has probably said "there's nothing quite like a cohort friendship," and if not, then I'm saying it now. Thank you in particular to Dr. Shelby Boyd, Evyn Routh, and Sam Daigle (and Erin!) for being on this ride with me.

Collaboration is essential to research. This project would not have been possible without the rigorous and innovative work of Professor Ashley Brown and her group in the Biomedical Engineering Department at NCSU. Thank you to Professor Brown for her guidance, support, time, and effort on this project. Thank you also to Dr. Dan Chester for all his work and input on the microgel side of this project. I would also like to acknowledge and thank Professor Kurt Gothelf of Aarhus University for making a summer of research in Denmark possible.

Thank you to my professors, friends, and mentors from the University of Missouri. Professor Cooley, for giving me free reign of his lab. Brian Booton for *everything*: letting me join EXPRESS late and guiding me into the Fellows program, for the support, the conversations, the friendship, and reading my essays of texts. Drs. Mia Brown, Ashley Dame, and Alison Tamasi for taking me under their wings as awesome women in STEM, and as friends. Rachel Hough (she knows what she did) and Mary McClannahan, for being the pieces of my soul I didn't know I was missing, and Kaitlyn Kahle and Jo Bryan – Missouri Five forever.

I would like to thank Professor Himadri Pakrasi for trusting a green nineteen year old with the responsibilities of a laboratory technician, as well as for everything I learned while working in his lab. I would like to thank Dr. Maitrayee Bhattacharyya for encouraging me to apply for the position, and for looking out for me since I was approximately the size of a bean. Thank you to Dr. Michelle Liberton for teaching me the fundamentals of research science, and to everyone else in the Pakrasi Lab family for their inspiration and support.

Finally, I'd like to thank my family: all my aunts, uncles, cousins, and grandparents who have tirelessly cheered me on. My sister from another mister, Katie – thanks for always being with me even when we're on opposite coasts. A very special thank you to Brian, mom, and dad: there wouldn't be a me without you.

TABLE OF CONTENTS

LIST OF TABLES

LIST OF FIGURES

CHAPTER 1: INTRODUCTION

1.1 The Need for Nanotechnology

The properties of every material are dependent upon the arrangement of their smallest components. As we create more advanced or more specifically tailored materials, the need to understand and control the very building blocks of nature becomes ever more essential. One of the first descriptions on the potential of a new field wherein there is the ability to arrange things on small length scales, down to the atomic level, was given by physicist Richard Feynman at Caltech in 1959 in his talk "There's Plenty of Room at the Bottom." Feynman proposed that control at the atomic level could imbue materials with designated properties that might not be available otherwise [1].

In the decades since Feynman gave this lecture – which everyone who has ever taken an interest in nanotechnology has encountered time and time again – techniques for controlling material properties at smaller and smaller length scales have emerged and improved rapidly. On their own, atoms are not able to be programmed to encode their own assembly into non-natural higher order structures. One solution is biomimicry: in nature, biomolecules carry enough intrinsic information to induce molecular self-assembly [2]. This fact has led to expansions in applications of synthetic biology as well as the development of innovative biomaterials. In particular, DNA has provided incredible potential as a structural material for applications in biomedical engineering, electronics and photonics, and information storage [3].

The field of DNA nanotechnology is fairly nascent and growing rapidly. As a biomolecule, DNA has the advantage of biocompatibility as well as the capability for use with other promising biomolecules, such as RNA, proteins, peptides, and aptamers [4]. Of particular interest is the use of unique, molecularly self-assembled, higher order DNA nanostructures in

drug delivery and cellular interactions. Cell signaling is a complex process; intercellular communication networks form vast webs that are responsible for many essential processes such as development, cancer prevention, and wound healing [5]. Not only do cells signal chemically at the nanoscale, but they also are capable of sensing and therefore responding to changes in their environments at the microscale through the mechanical properties of their surroundings in a process called mechanotransduction [5].

The complex interplay between these chemical and mechanical factors – i.e. where does one become more weighted in cellular response, how do they inhibit or enhance one another, and so on – is difficult to parse, partially due to the vastly differing length scales at which the processes occur [6]. Understanding these interactions would be an important leap forward in treating tissue disorders, from arthritis to conventional cuts and scrapes. Therefore, there exists a need for a multiscale tool that can bridge the gap between chemical and mechanical aspects of cell signaling.

DNA origami is a technique in DNA nanotechnology wherein a long, single strand scaffold is folded by shorter oligonucleotide staples into programmed shapes through thermodynamic self-assembly [7]. The origami shapes are programmable at the molecular level, but can also operate across length scales, making them unique tools for multiscale applications. In this project, a rectangular origami shape was functionalized at discrete sites in order to a) bind to a microgel substrate that mimics human tissue scaffolding and b) present a peptide sequence that targets a select cellular receptor. The viscoelastic properties of the microgel substrate can be tuned via chemical crosslinking, mimicking changes in mechanical properties that cells would experience *in vivo,* and the clustered peptide should, in theory, improve the reception of a target signaling compound – in this case, TGF-β [5]. It is expected that by presenting patterned peptide

to cells, and by adjusting the viscoelastic properties of the microgel thin films, cell proliferation and adhesion can be controllably modulated.

1.2 DNA Origami

DNA is an ideal structural material for nanofabrication because of its programmability, which comes from thorough understanding of its structure and behavior. The four bases of DNA – adenine, guanine, cytosine, and thymine (A, G, C, and T respectively) – pair selectively: A with T and C with G, forming base pairs (bp). Each of these is linked to a 5-carbon deoxyribose and phosphate backbone. The base, sugar, and phosphate groups together form nucleotides, which in turn give DNA its unique double helix structure [8].

The geometry of the base pairs can be described by six coordinates, which precisely define the location and orientation of every base – or base pair – in space relative to the previous unit along the axis of the double helix. These coordinates are: shift, slide, tilt, rise, roll, and twist [9]. The ability to so thoroughly describe the geometry of DNA is essential to its folding predictability. Additionally, three different structures of double helix occur in nature; for the purposes of this project, all references are to B-DNA [10].

B-DNA is right-handed, with approximately 10.5 bp per turn. The rise (bp along the axis) is approximately 0.332 nm long, and the pitch (helix turn) is approximately 3.32 nm in length. The diameter perpendicular to the axis is 2.0 nm [10]. These dimensions present minimum size scales, below which it is difficult to pattern using DNA nanofabrication.

Due to the extensive characterization of its structure and binding behavior, DNA is programmable, i.e. changing the sequence of base pairs changes the information that the DNA stores as well as its geometric properties. The process of molecular self-assembly is essential to the method of tailoring DNA.

Self-assembly is the arrangement of disordered, pre-existing units into a higher order structure that is determined by short scale interactions which determine which parts of which units will bind [2]. If these interactions are understood, they can be treated as code-able – where combinations of pre-existing units will form a predetermined higher order structure. The process is reversible by definition. Biological self-assembly is of concern in the scope of this project; this specific case involves biomolecular interactions of proteins and oligonucleotides. Of particular relevance to this process are hydrogen bonding, π-π stacking, van der Waals forces, hydrophobicity, and electrostatic interactions [3]. Hydrogen bonding controls base pairing and π-π stacking drives hybridization [10]. DNA self-assembles along pathways of thermodynamic favorability. The ends of a strand of DNA are less stable due to π-π stacking, which is also why longer strands are more stable than shorter ones. Mismatches reduce the energy, which means that imperfect sequence matches are unfavorable when the correct complement is available [11]. This property, as well as the extensive understanding of DNA's chemical and physical properties, allowed for the emergence of structural DNA technology.

Matching of strands with complementary sequences, called Watson-Crick-Franklin pairing, is one dimensional and therefore incapable of providing the structural diversity to make it a useful building material [10]. A stable branching system is essential to forming higher-order structures. The Holliday junction is essential to the use of DNA as a structural material since it provides this missing piece by binding two helices in predetermined locations [11]. An intermediate structure in genetic recombination comprised of two double helices that form a four-armed branch, the Holliday junction is unstable in nature [11]. Thus, in 1982, Nadrian Seeman proposed oligonucleotide sequences that were capable of forming a junction that was incapable of branch migration. It was still unstable, but several years of experimentation

provided the solution in the form of double crossover tiles, in turn allowing for the nascent field of DNA nanotechnology to emerge [12]. This comparison can be seen in Figure 1.1.

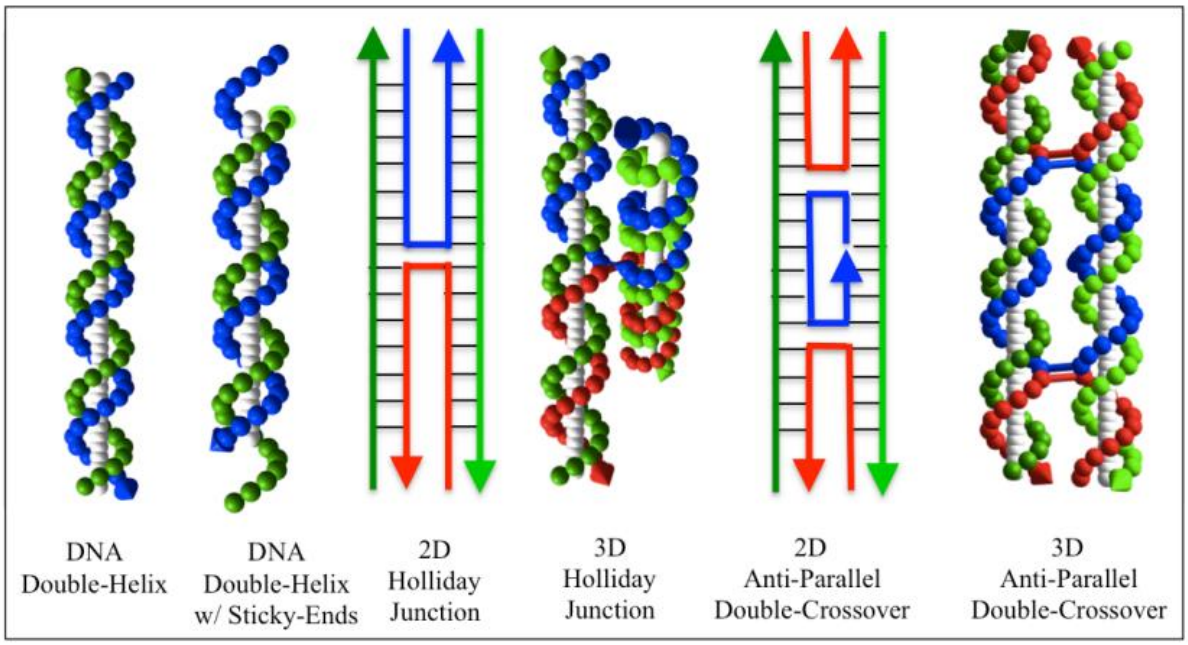

Figure 1.1: Visual representations of the DNA double helix, Holliday junction, and double-crossover, reproduced from Pederson et al. [13].

Of particular importance to this project is the technique of DNA origami, which was first described by Paul Rothemund in 2006 [7]. DNA origami, as subsets of DNA nanotechnology, are traditionally folded from the ~7,249 nucleotide single strand circular phage DNA extracted from the bacteriophage M13mp18, designated the ssM13 scaffold strand. This scaffold is directed into discrete shapes by any number of short single strand oligonucleotides, designated as staple strands. The folding occurs because the staples contain numerous crossovers, which force disparate regions of the scaffold to bind together, and ultimately to route correctly [7]. Rothemund demonstrated the versatility of this technique by folding a variety of shapes, shown in Figure 1.2 [7]. This project utilizes a functionalized derivative of Rothemund's original

rectangle design.

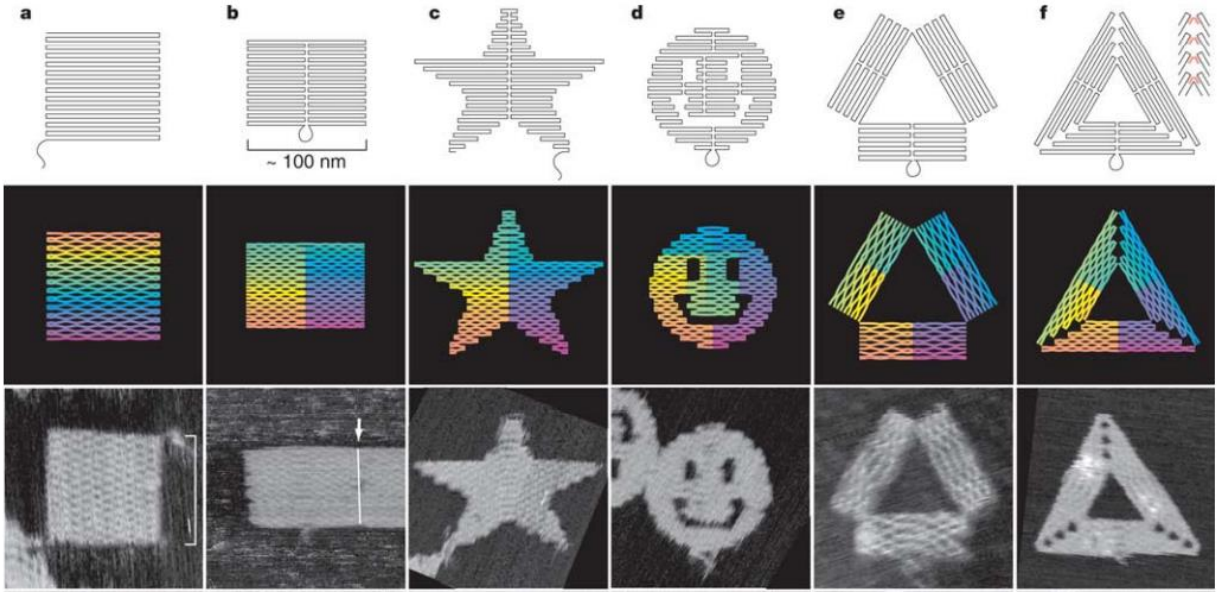

Figure 1.2: Unique DNA origami shapes, shown as rastering models and AFM micrographs. Note a) in particular, as it is the design used in this project. Figure reproduced from Rothemund et al. [7].

Due to the binding predictability and programmability of DNA, origami can be functionalized with molecular precision [14]. This is done via extension of staple strands and conjugation to either new sequences in the one pot folding reaction or addition of functional groups via proprietary commercial methods to either the 5' or 3' end of the staples. Since each staple is of unique sequence and unique location, the sticky end or functional group can be addressed to a specific location on the structure. This capability for precise and accurate functionalization at the molecular level makes DNA origami an ideal platform for the presentation of active biological groups to target receptors [15].

1.3 Peptides

Peptides are biopolymers consisting of 2-50 amino acids, making them smaller than proteins by definition, although both are polypeptides or poly-amino-acids [16]. Peptides are of an interest to the biomedical field because they either are natural ligands or can be substituted for

them, which interact with the receptors on cells. This gives peptides the potential to be more precisely targeted than conventional, small molecule drugs, and in the case of DNA nanotechnology provides the potential for more precise and accurate interactions between the DNA construct and its designated target [17]. DNA nanotechnology can further improve this targeting by controlling spatial arrangement of peptides, allowing larger scale recognition. Additionally, due to their smaller size, peptide folding is more controllable than that of proteins, and as reagents they are less expensive to manufacture [17].

Peptide nucleic acids (PNA) are synthetic polymers which were discovered in the early 1990s and are similar in structure to DNA and RNA [18]. Instead of a ribose-phosphate backbone, they have an N-(2-aminoethyl)-glycine backbone, with units linked by peptide bonds. Because this backbone has no phosphate groups, and therefore lacks their dense negative charges, the PNA/DNA strand binding is stronger than DNA/DNA strand binding due to the elimination of electrostatic repulsion, so the complementary regions can be shorter [18]. Furthermore, solid-phase peptide chemistry enables co-linear synthesis, which improves final product yield and purity [18].

These characteristics combined made PNA based targeting a logical choice for the scope of this project. A peptide sequence that recognizes the TGF-β receptor was chosen from literature [19]. This particular peptide sequence was selected because it binds non-agonistically and non-antagonistically to the TGF-β receptor, meaning that its presence should theoretically have no effect on TGF-β binding at all. Furthermore, the chosen sequence had been successfully implemented in previous studies involving spatial control of cells [19]. An oligonucleotide sequence complementary to strand extensions at selected sites on a DNA origami structure was added to the peptide sequence. This design is further discussed in the Methods section.

1.4 Wound Healing and TGF-β

TGF-β plays an essential and extensive role in traditional cutaneous wound healing. The wound healing cascade is comprised of four stages: hemostasis, inflammation, proliferation, and maturation [20].

In hemostasis, platelets begin to stick to the injured site and release chemical signals to initiate clotting. This activates fibrin, which holds platelets together, forming the clot itself.

In inflammation, damaged cells are removed and platelet derived growth factors are released, causing the migration and proliferation of cells.

In proliferation, new blood vessels are formed, collagen is deposited, fibronectin is released, and a new extracellular matrix is formed.

In maturation, unnecessary cells are removed, collagen aligns along lines of cellular tension, and the new tissue regains its former strength [20].

While this model of wound healing is divided into four phases, in reality there is considerable overlap between them [20]. Timing is essential, or else either significant scarring can occur or the wound never properly heals, resulting in a chronic wound [21]. As shown in Figure 1.3, TGF-β is involved in every major stage of the wound healing process, either directly or indirectly, and is partially responsible for cell migration, proliferation, and adhesion [20]. Furthermore, previous studies have shown that TGF-β activation changes in response to substrate viscoelasticity [22]. This makes it an ideal target for investigating the interplay between chemical signaling and mechanotransduction, since interfering with – or optimizing – TGF-β signaling has downstream effects on almost all of the chemical cascades in the wound healing

process, and should result in visible changes to cellular morphology [21].

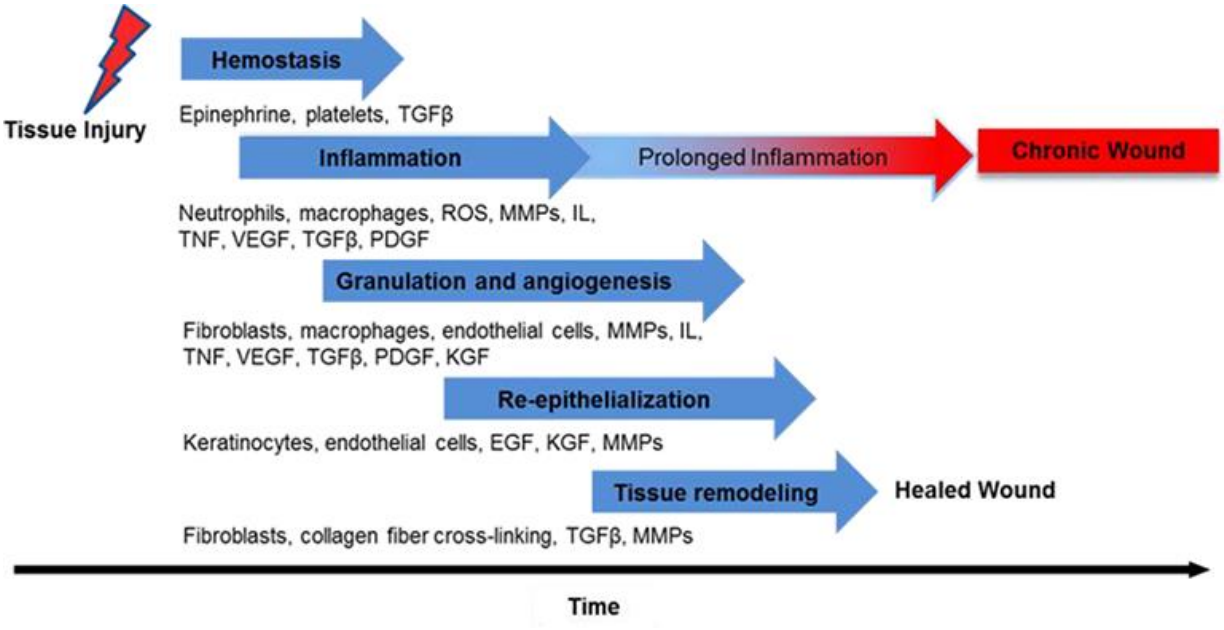

Figure 1.3: Flow chart of the stages of wound healing with relevant signaling factors. TGF-β is present in every stage of the wound healing process. Reproduced from Nguyen et al. [20].

Controlling the TGF-β response is essential to controlling proper wound healing. TGF-β is involved in balancing the levels of fibrin, fibrinogen, and fibronectin during the wound healing process, which is integral to preventing chronic wounds or excessive scarring [21]. If the TGF-β signaling pathway can be externally controlled, then this opens opportunities for innovative wound healing therapies.

The presence of TGF-β promotes dimerization, and is thought to promote oligomerization – clustering of the receptors has been linked to activation of the receptor's cytoplasmic phosphorylation domain [23]. The precise relationship between receptor clustering and kinase domain activation remains somewhat in question, therefore, the multiscale toolkit we develop here may also serve to clarify the steps involved in the TGF-β signaling pathway. From previous studies it appears that directed pre-clustering using antibodies, ligands, or some similar biomolecule by presenting them to the cell would sensitize the cells to the presence of TGF-β

[24]. In fact, previous work clustering TGF-β receptors with nanoscale precision using DNA origami and patterned affinity peptides has resulted in measurable changes in downstream analytes, specifically Smad proteins [24]. This work indicated that pre-clustering of TGF-β receptors by peptide presentation on origami sensitizes the cells to the presence of TGF-β, as the cells responded to a lower concentration of TGF-β than they would naturally. Therefore, it can be assumed that DNA origami and PNA-peptide can be successfully used to probe TGF-β signaling in the present work.

DNA origami can also bridge the gap between chemical signaling and mechanotransduction. Oligonucleotide extensions on DNA origami can be functionalized to hybridize with a complementary sequence that is attached to a select PNA-peptide which non-agonistically targets the TGF-β receptor. This pre-patterning should sensitize the cells to the presence of TGF-β. Similar extensions can be functionalized to covalently bind to a target substate that mimics tissue scaffold. For this project, the chosen substrates were colloidally stable microgel thin films with non-linear viscoelastic properties. Viscoelasticity has been recognized as a mechanical property which influences mechanotransduction; human tissue also displays non-linear elasticity [25,26]. For this project, high-tangent loss can be thought of as "less stiff" and low-tangent loss can be considered "stiffer" – mechanical properties which are tuned in the chosen microgel system through chemical crosslinking. These properties have been thoroughly characterized in previous work by collaborator Professor Ashley Brown's group in the Biomedical Engineering Department at North Carolina State University, we well as others [5,27,28]. Furthermore, studies have shown that these microgels can be used to directly observe receptor dimerization [29]. Tuning the viscoelasticity of the films via chemical crosslinking

between particles simulates the mechanical properties that influence cell adhesion, growth, and proliferation through mechanotransduction [5].

Between the patterning of PNA-peptide to increase the efficiency of TGF-β signaling and control of the film's viscoelasticity, cell adhesion and proliferation can theoretically be modulated, allowing the investigation of the interplay between chemical signaling and mechanotransduction.

1.5 Design Summary and Expected Outcomes

It is expected that, when in the presence of TGF- β, less stiff (1% BIS) films will cause cells to display more adhesion and spreading than the stiffer (7% BIS) films, in part because it is suspected that the cells have greater mobility on less stiff substrates. It is also expected that, regardless of film stiffness, pre-patterning receptor clustering at the nanoscale, i.e. samples with the full DNA origami multiscale tool, would result in a greater response to the presence of TGF-β, seen in increased area and decreased circularity of the cells. Random distribution of the peptide on the surface of the films – patterning at the microscale – are expected to yield results similar to what is seen in the unfunctionalized stiffer (7% BIS) films, since random patterning of peptide on the substrate would correspond to even more random clustering of TGF-β receptors than normal on the cell surface. Increased adhesion and spreading correlates to increased TGF-β sensitization. In the absence of TGF-β entirely, or in the case of being below the signal threshold, samples on microgels are expected to respond similarly to unfunctionalized films. A negative control in the form of a glass coverslip was also used; cells adhere and spread rampantly on glass. Figure 1.4 summarizes the components of this project, the patterning types, and expected outcomes.

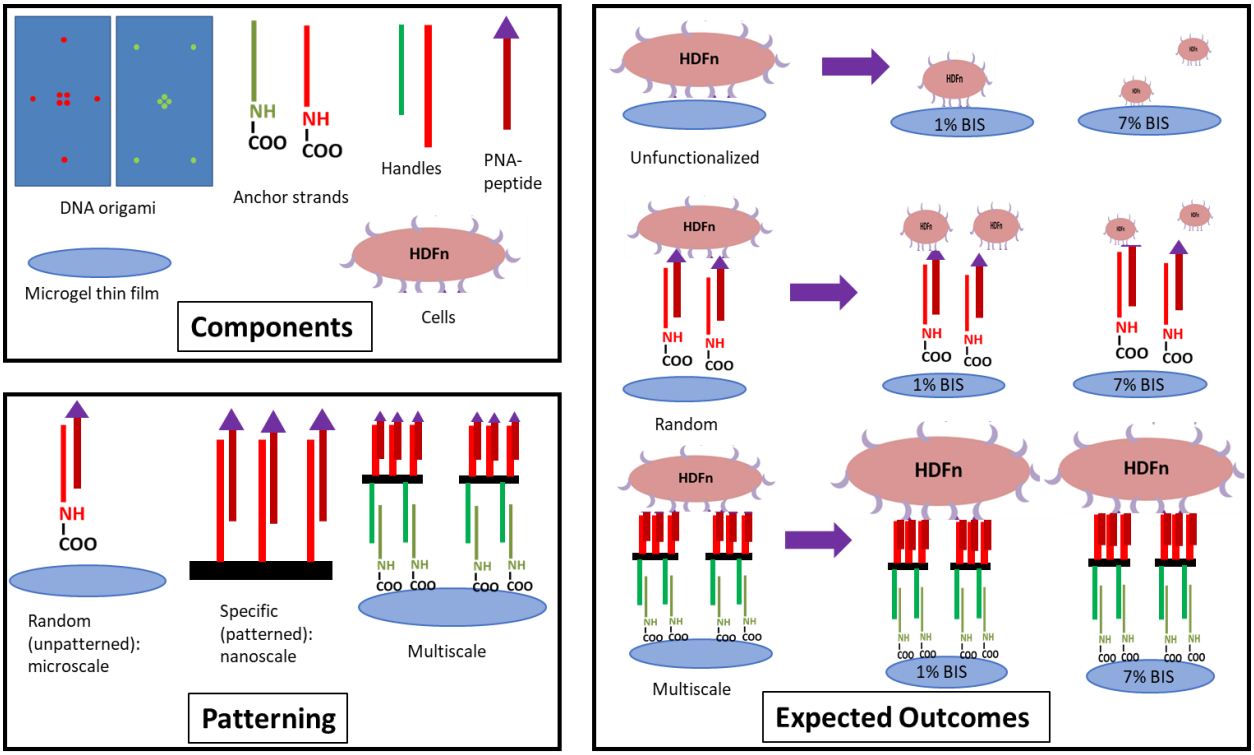

Figure 1.4: A simplified visual summary of the components, patterned arrangements, and expected outcomes of this project. All outcomes shown are expected to occur in the presence of TGF-β, although the signal input is not shown. Note the color coding between replacement sites, oligonucleotides, and their complements (red and green), as well as the peptide (purple triangle) and TGF-β receptors on the cell surface (crescents). Images are not to scale.

The components of this design, including synthesis and analysis of the tool itself, will now be discussed in more detail.

CHAPTER 2: METHODS

2.1 Microgels

The microgels were comprised of poly(N-isopropylacrylamide) (PNIPAm) based particles, which were synthesized in the lab of Dr. Ashley Brown using standard precipitation polymerization [30]. In order to give the particles a negative charge and provide acrylate groups for functionalization, acrylic acid (AAc) was copolymerized with the PNIPAm at a constant 5% molar ratio. N,N'-methylenebis(acrylamide) (BIS) was used as a crosslinker to tune the stiffness of the microgels. Uncrosslinked, 1%, 2%, and 7% BIS crosslinked microgels were used, and eventually 1% and 7% BIS films were chosen under the assumption that they would provide the most drastic differences in cell behavior compared to each other, based upon results from a different project in Dr. Brown's lab.

The microgel thin films investigated were multilayered, and were fabricated in a layer-by-layer process using active centrifugal deposition [31]. The multilayer films had four layers, with each layer of microgel particle solution alternated with poly(ethyleneimine) (PEI). PEI is positively charged and the polymer particles are negatively charged, so the PEI acted as an electrostatic glue to hold neighboring particles together. The films were deposited onto glass coverslips. Once deposited, the dry films were stored at room temperature.

2.2 DNA Origami Design

The origami chosen was Rothemund's original rectangle design, as it has been extensively characterized. It was not twist corrected, since previous works have suggested that one side of the rectangle is more likely to deposit face down on a substrate [32]. This trait was considered a potential benefit to the design of the tool, as it increases the likelihood of origami presenting the correct sticky ends down to the substrate and up to the peptide.

The original design staples, listed in Appendix A, all ended on the same side of the origami, making splicing them necessary in order to curve around to the other side of the helix in select locations. The thorough existing characterization of the rectangle design allowed for straightforward selection of staple strands to splice and extend. As a consequence of the strand splicing, fractional staples were created.

As shown in Figure 2.1, one side of the origami, designated 'O,' was designed to face downwards toward the microgel film substrate. Eight different staple strands were chosen for extension: four distal to the center of the origami and four proximal. These locations were assumed to be sufficient for providing stable attachment to the substrate. The full list of replacement staples can be found in Appendix B.

The other side of the origami, designated 'P' and designed to face upwards, presents eight different sites, slightly offset from the O sites but similar in relation to the center of the origami, that are meant to hybridize with the oligonucleotide tail on the P-PNA-peptide, the sequence of which can be found in Appendix C. The peptide in turn binds to the TGF-β receptor on neonatal human dermal fibroblasts (HDFn). The P sites were chosen at locations which were thought to provide several options for receptor clustering in terms of geometric distance. The previous work by Pedersen et al. had indicated that sensitization could occur from clustering in the lower distance range, i.e. the arrangement at the center of the origami, but it was of interest to provide some regions further apart as well. The current scope of this project involved functionalizing every site without regard for determining the optimal geometric arrangement, but this design allows for sites to be used or omitted depending upon which staples are replaced with the functional extension.

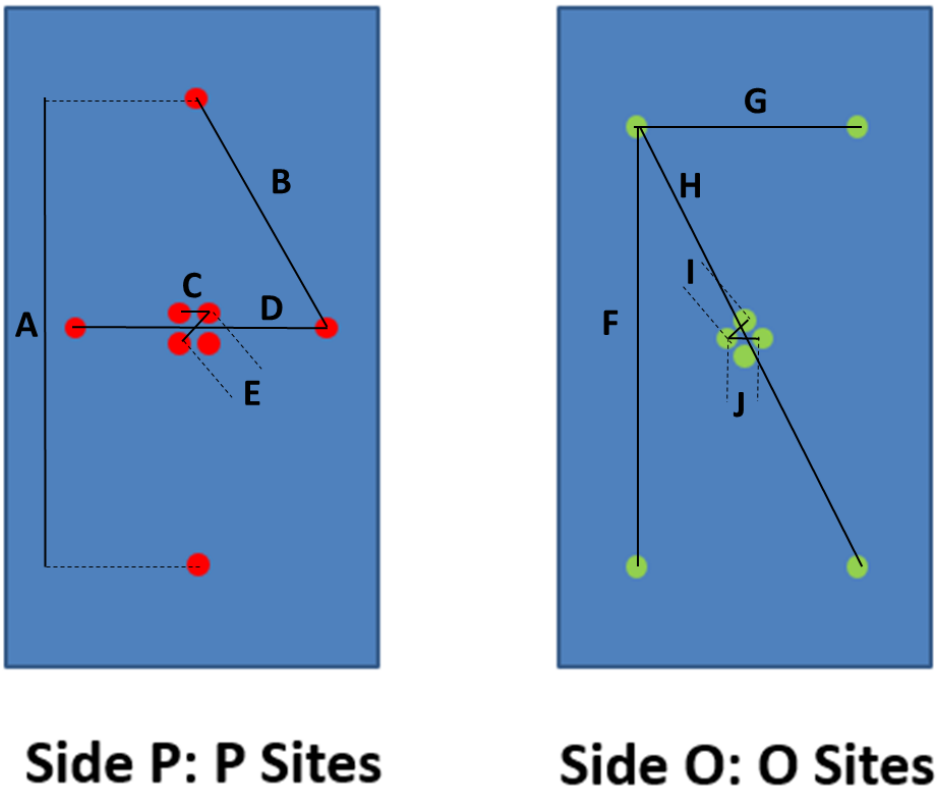

Figure 2.1: Representative locations of replacement sites on origami with distances of approximately A) 32 nm, B) 19.4 nm, C) 4 nm, D) 22 nm, E) 5.6 nm, F) 24 nm, G) 22 nm, H) 32.6 nm, I) 2.8 nm, and J) 4 nm.

The sixteen total sites were created by splicing original staple strands from Rothemund's rectangle and including extensions that are conjugates of the respective target oligonucleotides.

The O staple extensions were designed to conjugate to O* Anchor strands. The O* Anchor is functionalized on the 3' end with an amine group in order to covalently bind to carboxyl groups within the microgel substrate.

The P* staple extensions hybridize with a unique, complementary oligonucleotide sequence on the P-PNA-peptide. This allows for the peptide to be presented to cells, localizing to the TGF-β receptor in a non-agonistic, non-antagonistic manner. Additionally, a P* Anchor – functionalized with the same amine group as the O* Anchor, but on the 5' end – was designed in

order to investigate any differences between patterning peptide on the origami (i.e. nanoscale clustered) and patterning it on the microgel substrate directly (i.e. unclustered).

In order to determine if the origami properly binds to the microgel substrate as designed, a fluorescently-labeled P Probe strand complementary to the P* Handle (the sequence of which can be found in Appendix C) was also designed and synthesized. This assay will be further described in Section 2.3.6.

The full tool is visualized in reduced form, and not to scale, in Figure 2.2. Only one O* Anchor and corresponding O Handle are shown in order to reduce visual confusion, for instance, and the O Handle is not shown at precisely an O site. However, it serves to illustrate how the component parts – the microgel substrate, the aminated O* Anchor hybridized to the complementary O Handle, the DNA origami, the P* Handle extension and its complement within the P-PNA-Peptide – present the peptide to the cell in order to pre-cluster receptors that would normally be patterned randomly across the cell's surface.

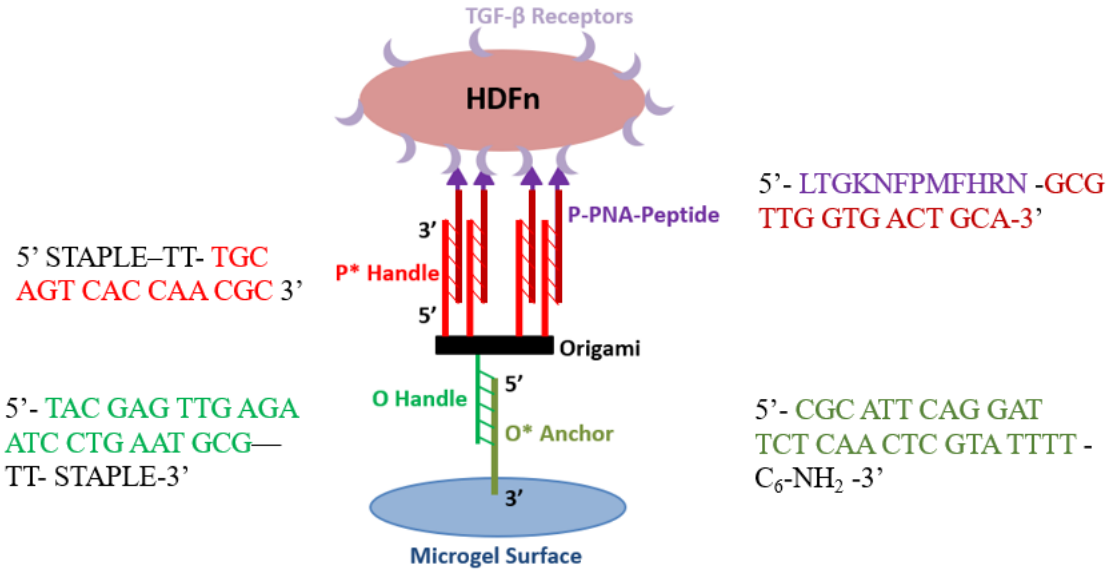

Figure 2.2: Reduced form representation of the multiscale tool design. Note the color-coding between complementary sequences. Full sequences for all sites can be found in Appendix B.2.

2.3 Protocols

2.3.1 Preparation of DNA Origami

A one pot hybridization assembly reaction of 9 nM rectangular origami was prepared according to conventional methods [7]. Briefly, the 200 μL anneal was prepared in 1X TAE-Mg^{2+}, pH 8.6 (40 mM Tris base, 20 mM acetate, 1 mM EDTA) buffer; the positive charge from the divalent Mg cations is necessary to maintaining the shape and stability of the origami, since DNA has a negative charge. The added magnesium has a concentration of 12.5 mM and comes from the addition of magnesium acetate. Staples were added in 10x excess, and the reaction was annealed in a stairstep process from 80°C to 20°C for sixteen hours. The anneals were spin filtered according to traditional methods, with three rinse steps using 1X TAE-Mg^{2+}. Folding was confirmed using atomic force microscopy (AFM) on origami samples deposited on mica.

2.3.2 Oligonucleotide Conjugation to Aminated Microgels

Films were kept on glass coverslips in twelve well plates, and prior to activation were sterilized with 1 mL each of 70% ethanol by incubating at 2°C overnight. 1 mL of 10 mM MES buffer, pH 4.7, was added to dry films in order to rehydrate them, and incubated at room temperature, shaking at 100 rpm for 30 minutes. The MES buffer was then removed from the films.

A master mix of 12 mg/mL 1-Ethyl-3-(3-dimethylaminopropyl)carbodiimide (EDC) and 7.5 mg/mL N-hydroxysulfosuccinimide (sulfo-NHS), was prepared in 10 mM MES buffer, pH 4.7. This activates the carboxyl groups on the particles within the films, which allows them to couple to amine groups. 1 mL of the mix was added to the films in the well plates, and incubated at room temperature for two hours, shaking at 100 rpm.

The films were then rinsed three times with 10 mM MES buffer, shaking at room temperature and 100 rpm for 5 minutes on each iteration. The films then incubated at room temperature in 18 MΩ water for 30 minutes in order to remove any MES buffer that may have intercalated between particles or layers.

The O* Anchor strand was added to 1X TAE-Mg^{2+} buffer for a final total volume of 1 mL per well. The O* Anchor added was calculated to be at a 10:1 molar ratio the acrylic acid on the microgel particles. In other words, the film types (1% and 7%) receive a different concentration of O* Anchor, but each sample well still receives 1 mL of final solution. The same was done for P* Anchor, for the randomly patterned peptide controls (still with 1 mL final total volume per well). The films were then incubated at room temperature, shaking at 100 rpm, for 2 hours.

2.3.3 Addition of DNA Origami and Peptide to Films

The origami anneal was deposited with the additional volume of P-PNA-peptide added in order to attain a final concentration of 5 nM peptide in 1 mL of solution per well. The samples were incubated at room temperature for 2 hours, shaking at 100 rpm. They were then washed three times with 1X TAE-Mg^{2+} buffer, shaking at 100 rpm for five minutes per wash.

The films were then coated with 1 mL of 20 μg/mL fibronectin (FN) by incubating overnight at 4°C. Fibronectin enhances initial cell attachment to the substrates, improving initial seeding conditions and preventing colony crash [5]. The samples were then washed three times with 1X PBS in the same manner as previous washing steps.

2.3.4 Culturing and Depositing HDFn Cells

Human dermal fibroblasts, neonatal (HDFn) were cultured in serum free Dulbecco's Modified Eagle Medium (DMEM) with 1X L-glutamine until approximately 80% confluent, or when spun down could yield 12k-14k cells/mL – the initial seeding concentration. The HDFn cells were removed from the substrate of their flask with trypsin, which was inactivated using serum-containing media. The cells were resuspended such that 12k-14k were added to 1 mL of serum free DMEM per well. TGF-β was added to the relevant samples five minutes after cell seeding, with a final concentration of 200 pM. This concentration of TGF-β was chosen from previous work involving pre-patterning TGF-β receptors [24]. Although the work of Pedersen et al. demonstrated that cells could be sensitized to a concentration as low as 40 pM TGF-β, it was decided that starting with a higher concentration was the proper course.

After a 24 hour incubation period at 37°C, cells were fixed with 95% methanol 5% acetone and stained using NucBlue. They were then imaged using an EVOS fluorescence microscope. After being fixed, samples were mounted to glass microscope slides by adding 10

μL of mounting medium to the fixed sample, gently pressing the sample side down onto a glass microscope slide, and then brushing nail polish around the edge of the coverslip to seal the sample. After setting, the samples were then stored at 4°C.

2.3.5 Sample Variants

Several different controls, positive and negative, were tested and compared in order to investigate cellular response. All samples were made in duplicate. All experiments involved a negative control of cells seeded onto a glass coverslip. Initial experiments were performed without FN coating films, but as shown in Figure 3.3, it was found that FN coating improved initial cell attachment. Quantitative analysis of the difference can be seen in the "Results" section of this thesis. In all subsequent experiments, a negative control of an FN coated glass coverslip was always present, as were FN coated films with no oligonucleotides, origami, or

peptide present.

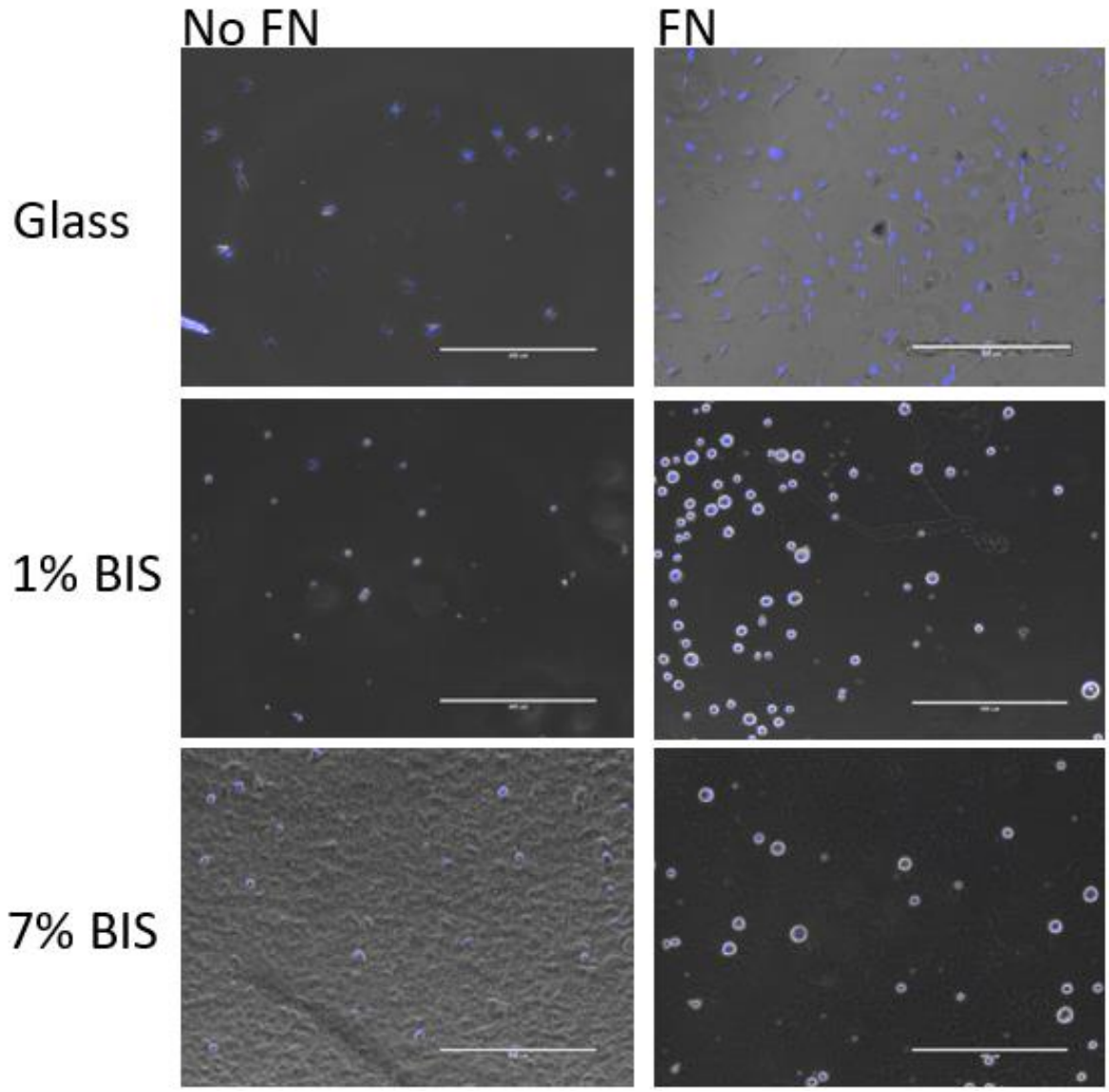

Figure 2.3: Representative images visually demonstrating a comparison of cells on glass coverslips, 1% BIS, and 7% BIS films without and with fibronectin. All scale bars are 400 microns.

During the process of optimizing the concentrations of origami, peptide, TGF-β, cells, and so on, cell samples were prepared at each stage of the assembly process in order to determine if appreciable differences could be seen with and without the PNA-peptide, with and without origami, with peptide patterned directly to the microgel substrate via the P* Anchor, and so on in

every possible permutation, shown in Table 2.1. The negative controls of only Anchor strands or unbound peptide consistently yielded results similar to the negative controls of cells on films alone, and were eventually phased out of the sample sets. The purpose of

Table 2.1: Description of sample types, their purpose, and which were deemed relevant to downstream experiments.

Sample Contents	Purpose	Kept in Later Experiments
Glass coverslip	Negative control – healthy cells should attach and spread	Yes
1% BIS monolayer films	Negative control – cells attach (not as well as on glass), but do not spread well	Yes
7% BIS monolayer films	Negative control – cells attach (not as well as on glass or 1% BIS films), but do not spread well	Yes
P* Anchor	Negative control – test of surface roughness/energy effect on cells	No
P* Anchor + P-PNA-Peptide	Negative control – peptide randomly patterned on film surface, without TGF-β	Yes
P* Anchor + P-PNA-Peptide (+ TGF-β)	Positive control – peptide randomly patterned on film surface, with TGF-β	Yes
O* Anchor	Negative control – effect of surface roughness/energy change on cells	No
O* Anchor + Origami	Negative control – effect of origami on cells	No
O* Anchor + Origami + P-PNA-Peptide	Negative control – full tool assembly without TFG-β	Yes
O* Anchor + Origami + P-PNA-Peptide (+ TFG-β)	Positive control – full tool assembly with TFG-β	Yes

including these to begin with was to determine if adding oligonucleotides to the surface of the microgels affected the cell sensing process – i.e. by way of changing surface roughness or surface energy – in any way, and to see if unbound peptide, free in solution, influenced cell behavior. Since the cells grew as if interacting with the films alone, it was decided that these negative controls were unnecessary. They will therefore not be discussed in relation to experimental results as they stand at the current state of this project.

Additionally, preliminary experiments used uncrosslinked, 2% BIS, and 7% BIS films, both monolayered and multilayered – the latter having four layers. Eventually, it was decided that 1% BIS and 7% BIS monolayers were most likely to provide the most explicit framework for clear differences in cellular response between high loss tangent and low loss tangent substrates due to initial findings from another ongoing projects in Professor Brown's group. Therefore, the 1% and 7% BIS monolayer results are most pertinent to this project and will be discussed in most detail.

2.3.6 Imaging and Image Analysis

Atomic force microscopy (AFM) was used to confirm proper origami folding. This was done by removing the staples that were to be replaced in one sample, and adding the altered staples back in the other sample, with the results seen in Figure 2.3. Imaging was performed in tapping mode on liquid samples mounted on mica in the presence of divalent cations (Mg^{2+}). Origami bind well to negatively charged mica with the addition of the cations, which also help to maintain the structure of the origami during imaging. The resulting images confirm staple replacement but not necessarily end location; in the future, it would be beneficial to either functionalize the target sites on both sides of the origami with gold nanoparticles, or with a

biotin/streptavidin linker, as both can be visualized with AFM.

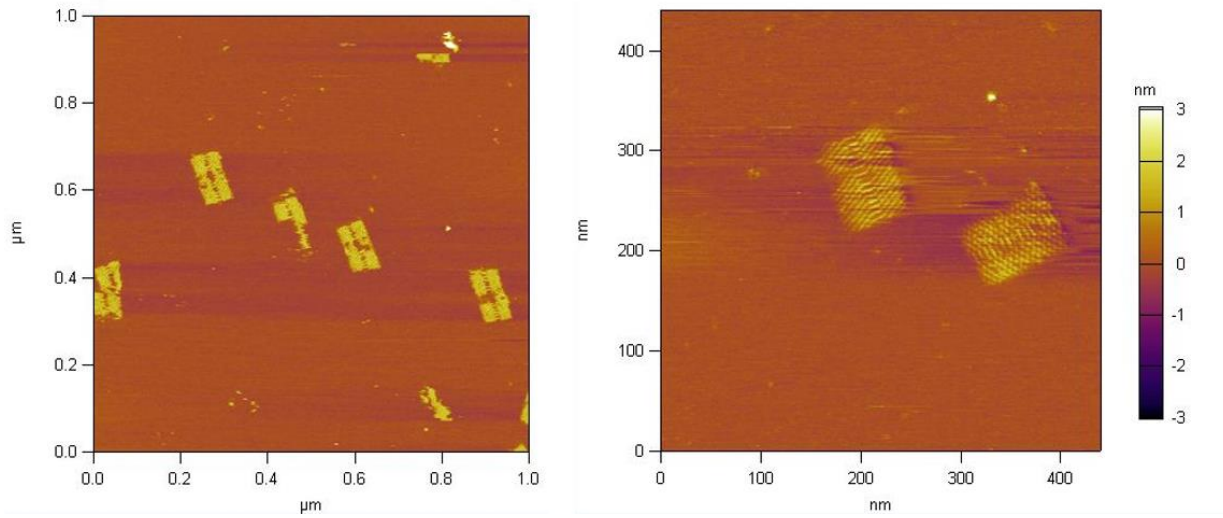

Figure 2.4: AFM micrograph of origami samples representing removed staples (L) and replaced staples (R). The right hand image shows the holes seen in the left hand image, caused by missing staples, to be eliminated.

In order to determine if the origami were binding to the microgel surfaces, a rudimentary test was devised that involved covering half of a class coverslip with tape prior to depositing the microgel, thereby providing only a half surface for origami to bind. A probe strand with a sticky end complementary to the P* Handle of the origami – i.e. designed to bind at the same sites as the P-PNA-Peptide, facing upward on the origami surface – was designed and purchased. The fluorophore was Cy5. It was hypothesized that the region of the coverslip that had microgel film would fluoresce more brightly than the region that did not, for both 1% and 7% microgel films, since the P* Probe should bind to P Handle on the origami and fluoresce. The origami were deposited according to the protocol outlined above, and the samples were imaged on an EVOS microscope. Figure 2.4 is a representative image of the results. Although this method does not

quantify the number of origami bound to the surface, it does confirm origami binding in general.

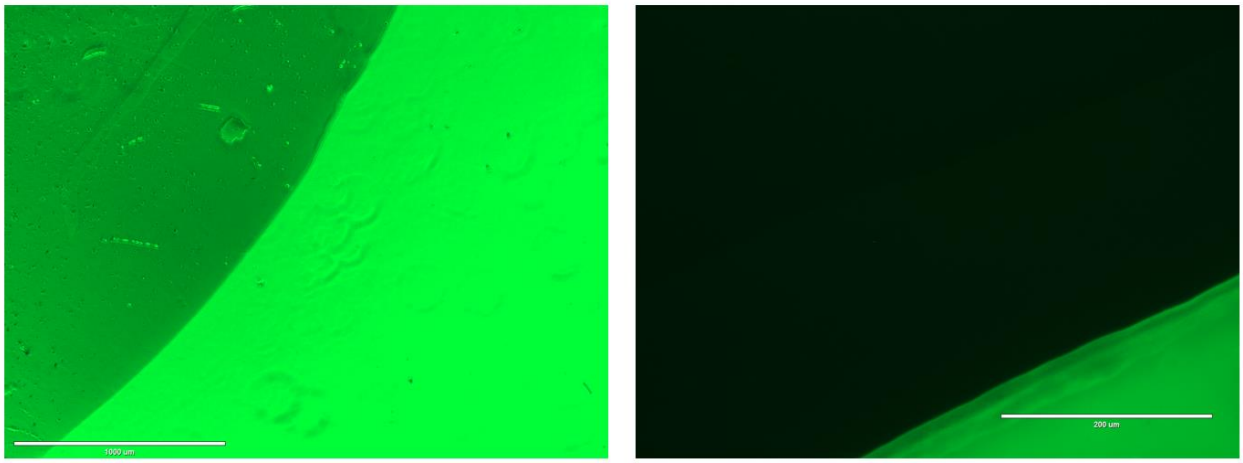

Figure 2.5: Fluorescent images of origami deposited on 1% (L) and 7% (R) BIS half films. The brighter regions in the lower right side of both images represent the areas with film and origami deposition. Left scale bar is 1000 microns and the right is 200 microns.

Nuclei of deposited cells were stained with NucBlue in order to make living cells more apparent while imaging. Area and circularity of cells in the samples was calculated from images taken on the EVOS using ImageJ. Images and representative data analysis can be found in Appendix D. "Circularity" is meant in the geometric definition of the word, i.e. the two-dimensional roundness of a cell. Increasing area and decreasing (i.e. closer to a null value) circularity correspond to strong adhesion and spreading. Cells that are not spreading are physically more circular. Disregarding the possibility of no cells attaching at all, on one extreme all cells wouldn't spread, and have lower area and higher circularity, and on the other extreme all cells would spread and have greater area and lower circularity. However, at least in the case of cells on films with the various experimental tool regimes, there is also the possibility of a bimodal, or blended, response. Figure 2.5 demonstrates this gradation visually: in the top panel, cells are almost perfectly circular, with lower cell area, and the cell count in the frame is low, indicating poor adhesion and spreading. The middle panel shows a bimodal response, with almost half of the cells highly circular – not spreading – and half with low circularity and high

area, i.e. adhering and spreading. The bottom panel shows cells with low circularity and greater area, indicating a high degree of adhesion and spreading. The quantitative ramifications will be discussed in the following section.

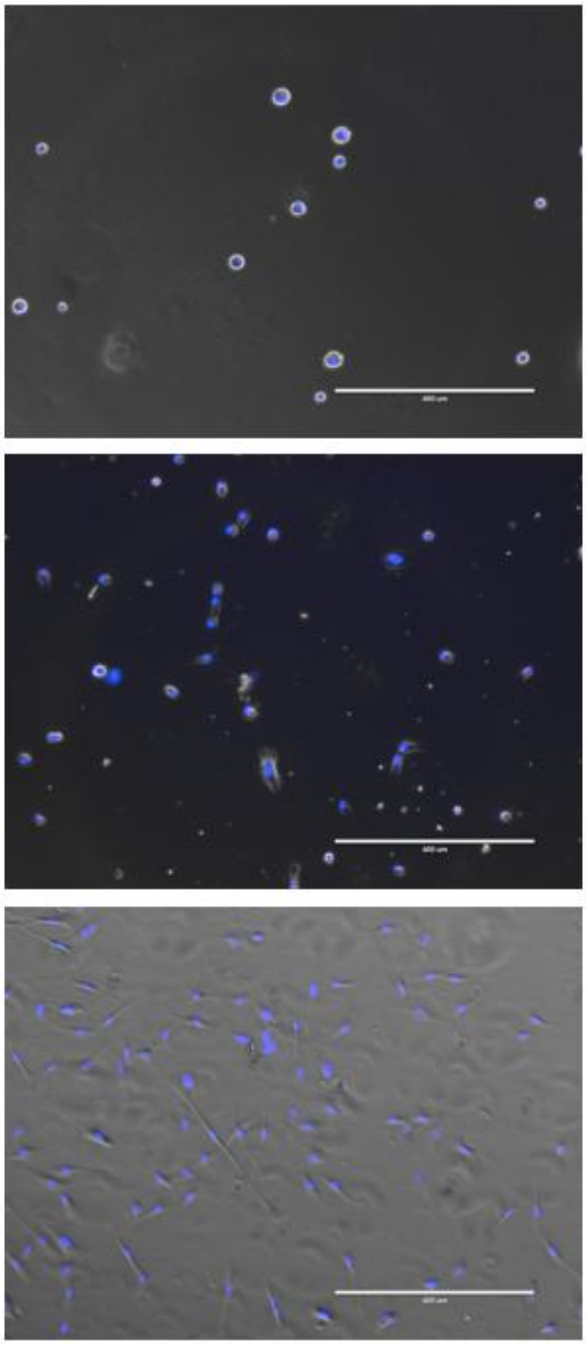

Figure 2.6: Representative images of attached cells that are low area and high circularity (top), bimodal (middle), and high area and low circularity (bottom). All scale bars are 400 microns

CHAPTER 3: DISCUSSION

3.1 Preliminary Results

It was initially hypothesized that pre-clustering of TGF-β receptors via PNA-peptide presented to cells on DNA origami would result in consistent and predictable trends of cell adhesion and proliferation. Similarly, it was expected that adding in the additional component of microgel monolayers of differing viscoelastic properties – the 1% BIS films are less stiff than 7% - would also result in predictable cellular responses.

It was expected that the less stiff (1% BIS) films would cause cells to display more adhesion and spreading than the stiffer (7% BIS) films, in part because it is suspected that the cells have greater mobility on less stiff substrates simply because they have more leeway to rearrange. It was also expected that, regardless of film stiffness, pre-patterning receptor clustering at the nanoscale, i.e. samples with the full DNA origami multiscale tool, would result in a greater response to the presence of TGF-β, seen in increased area and decreased circularity of the cells. Random distribution of the peptide on the surface of the films – the samples with P* Anchor and P-PNA peptide alone – was expected to yield results similar to what is seen in the stiffer (7% BIS) films. However, this was not entirely the case.

Firstly, experiments were initially conducted without FN coating samples. As shown in Figure 3.1 compared with Figure 3.2, the lack of FN resulted in poorer cell adhesion and, at least in part, greater standard deviations from the mean values. It was therefore decided to proceed with FN coating all samples. The negative controls mentioned in Table 2.1 that had been deemed unnecessary were also tested with and without FN, and as the cell behavior remained the same as on the glass substrate negative control, it was confirmed that they could continue to be removed from further experiments and the scope of this thesis.

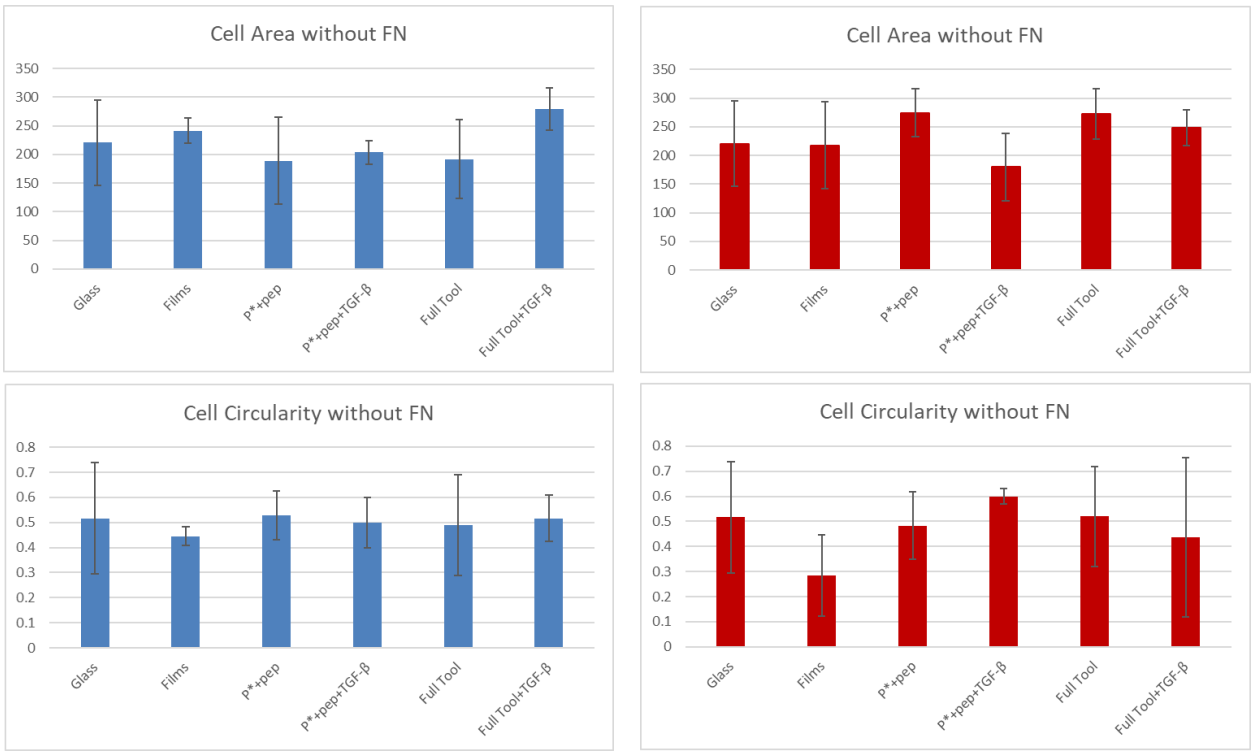

Figure 3.1: Area and circularity data of 1% BIS (left) and 7% BIS (right) crosslinked samples without FN coating. Error bars are standard deviation from the mean.

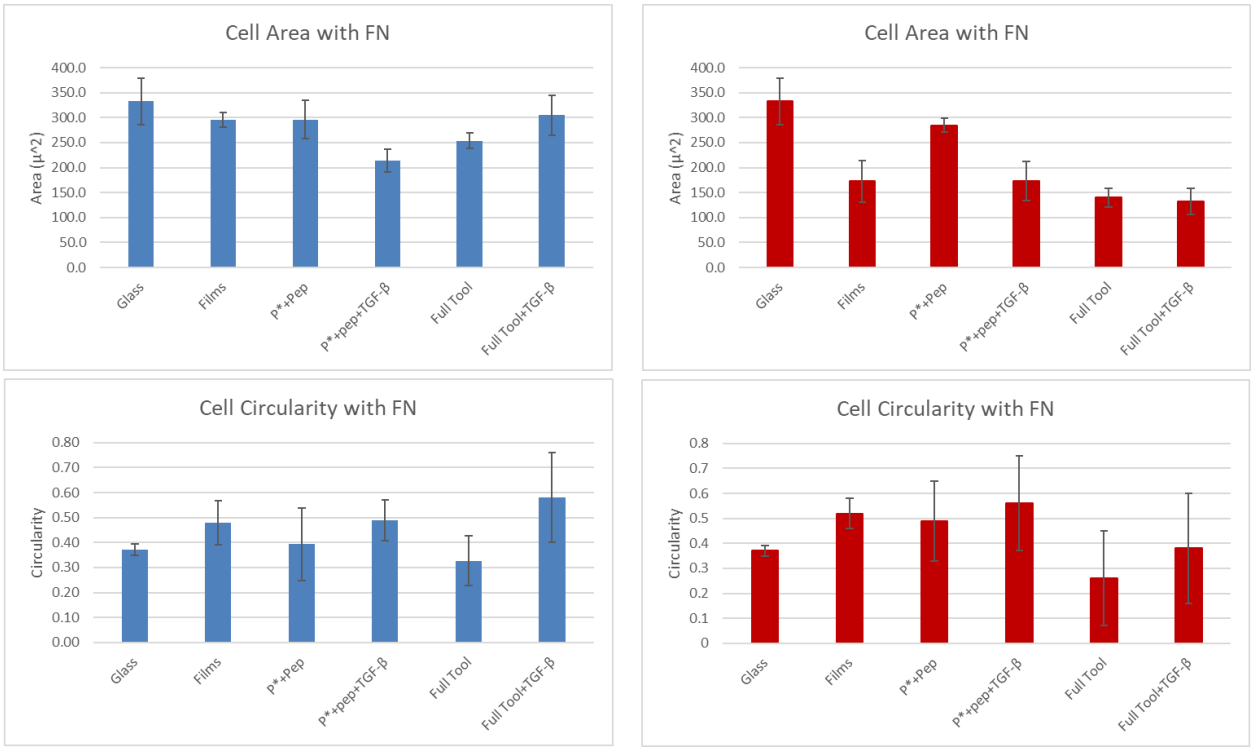

Figure 3.2: Area and circularity data of 1% BIS (left) and 7% BIS (right) crosslinked samples with FN coating. Error bars are standard deviation from the mean.

However, as subsequent experiments were conducted, results contradicted expected outcomes or, in most cases, did not produce replicable trends. For instance, the addition of the peptide and TGF-β frequently caused a decrease in cell adhesion and proliferation in both monolayer cases. Furthermore, the addition of origami in general decreased the likelihood of cell adhesion. Cells stimulated by TGF-β also didn't adhere to the monolayers as expected: where it was anticipated that 1% monolayers would yield higher rates of adhesion and proliferation in the presence of TGF-β, the opposite was more likely to occur. In this case, at least, it is suspected that the cells may be adhering so tightly that they are tearing the monolayers, and therefore failing to proliferate because they are not receiving the expected mechanical input from their substrate.

However, there is the possibility that these unanticipated results can be explained by a bimodal response in cell behavior. Cells frequently behave at opposite ends of a spectrum; that way, if their environment rapidly changes from one extreme to another, more of them are likely to survive [33]. In the case of this project, this would be seen as a portion of cells per sample adhering and spreading, and a portion doing nearly the opposite, with at least enough adhesion to survive. This nuance must be accounted for when quantifying results, as it can cause a misrepresentation of data without a visual to represent where cells are falling along this spectrum. Figure 3.3 illustrates this distinction. The distribution of data points at generally either end of the standard deviation, including some outliers, shows that the cellular response isn't a neat "spreading" or "not spreading" scenario. However, even with this accounted for, trends were difficult to replicate and occasionally contradicted expected outcomes.

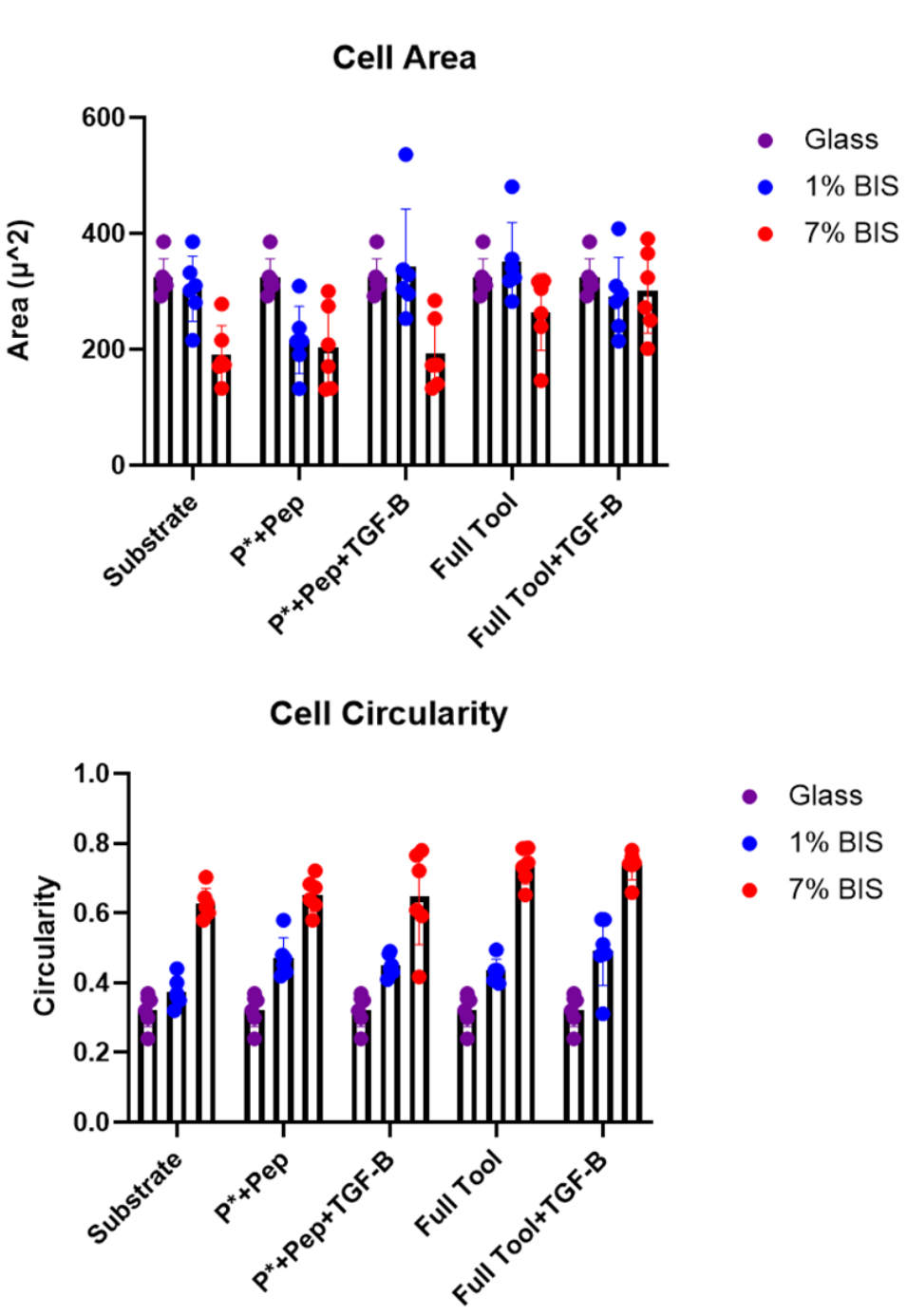

Figure 3.3: Representation of area and circularity data for cells on glass, 1% BIS crosslinked, and 7% BIS crosslinked films, including a visual of where cell colonies fall in the range of values.

Cells adhered and spread on the glass control substrate as expected, and consistently, indicating healthy cell cultures overall. However, it was expected that the less stiff (1% BIS)

films would have cells which display more adhesion and spreading that the more stiff (7% BIS) films, in part because it is suspected that the cells have greater mobility on higher tangent loss substrates: this result did occur, to a degree, at least to the extent that cells on 7% BIS crosslinked films were more circular – i.e. did not spread as much – as those on 1% BIS crosslinked films. However, there was little difference in cell area overall.

It was also expected that, regardless of film stiffness, pre-patterning receptor clustering at the nanoscale – samples with the full DNA origami multiscale tool – would result in a greater response to the presence of TGF-β. Preliminary results show little difference in response between pre-clustered and randomly patterned receptors. That is to say that current results are inconclusive as to whether or not pre-clustering TGF-β receptor on cell surfaces sensitizes the cells in this system to the presence of TGF-β.

Finally, random distribution of the peptide on the surface of the films – the samples with P* Anchor and P-PNA-peptide alone (the samples called P*+pep) – was expected to yield results similar to what is seen in the lower loss tangent (7% BIS) films. Current data is inconclusive as to that result: the cell area analysis suggests a similar response, whereas the circularity analysis indicates that cells on 7% BIS crosslinked films overall tend to spread less than their 1% BIS crosslinked film counterparts.

In general, more work must be done to investigate each discrete aspect of the interactions between the multiscale DNA origami tool, the microgel substrates, and the moving parts of the TGF-β, the cells, and the binding of the peptide, which is perhaps not surprising in a system this complex.

3.2 Challenges

The most difficult aspect of this project is that, by its nature, in order to ascertain if the DNA origami multiscale tool is binding and behaving as expected, interacting at both the microscale and the nanoscale, the methods used must confirm behavior across length scales. Attempts were made to confirm coverage of P* and O* Anchor strands on the microgel substrate via fluorescence microscopy, but due to the limitations of microscope resolution, no nanoscale precision could be achieved. However, exposing only one half of a film to fluorescent P* and O* Anchor strands did demonstrate greater fluorescence where expected.

In theory, functionalizing discrete sites on DNA origami with other chemical groups is fairly trivial, and this is often the case in practice – however, it is difficult to account for the effects of binding affinity. For instance, using a biotin marker to confirm the location of extended functional sites on both sides of the origami is possible, but does not guarantee that the carboxyl group added to the 3' end of the O* Anchor sequence does not in some way interfere with integration of those staple strands into the overall origami structure. Furthermore, it does not imply that the PNA-peptide, even with its oligonucleotide tail that is complimentary to the P* Anchor sequence presented upwards on the origami, binds as reliably as expected. Then, of course, there is the additional complication of analyzing all of these parts at once since the full multiscale tool only has relevant function when it is completely assembled.

This also does not account for behavior between PNA-peptide and the cells, or the cells and TGF-β, and all of the above with the DNA origami and the substrate itself.

CHAPTER 4: FUTURE DIRECTIONS

4.1 Process Engineering

The most essential step to continuing this project is to analyze all of the "moving parts" involved. As discussed above, the interaction between each component could have a significant impact on the outcome of cellular behavior, in part precisely because cells are so sensitive to their environments.

One potential solution to the issue of determining coverage – both of P* Anchor in relation to PNA-peptide patterned randomly onto the microgel surface as well as the density of coverage of DNA origami to the surface itself – is the DNA-PAINT technique [34]. DNA-PAINT uses short, dye-labeled single strand DNA probes that interact transiently with their complement-attached targets; the brief interactions provide the intermittent signal for high-resolution imaging. This could at least provide the resolution to get a broad sense of what is binding and where: the microgels are not flat at the nanoscale, since they are formed from particles in colloidal solution; there is a possibility that the curvature of the particles is interfering with origami binding to the film surface. Additionally, as mentioned earlier in this document, functionalizing both the O and P sites with gold nanoparticles or a biotin/streptavidin linker would allow visualization via AFM of staple site replacement and allow a more accurate count of binding consistency.

Other geometric factors should also be considered, such as possible entanglement between Anchor strands, which could inhibit binding. The current design of the P sites allows for preliminary exploration into these factors without having to alter the design of the origami.

Additionally, the arrangement of O Anchor on the origami was only assumed to provide stable binding of origami down to the films; this might not be the case. If the interaction was too

weak, then the full tool could be washed off before they are able to affect the cells. Other configurations of strands that bind the origami to the substrate surface could be explored.

There is also a possibility, suggested from previous origami-cell interaction studies, that the cells are ripping the origami apart when they bind to the substrate. Finally, because TGF-β is intrinsic to several different cascades that determine cell proliferation, migration, adhesion, and so on, it could be that interfering with the TGF-β signal on such a broad and directed scale is causing unanticipated downstream effects, such as apoptosis. One way to test this would be to target other receptors on the cell surface.

4.2 Other Targets on the Cell Surface

Even after the intricacies of the TGF-β exploration are solved, it would be interesting to approach other major cell surface receptors in a similar manner. Other growth factors such as PDGF, FGF, and VEGF could potentially be targeted, as could cytokines such as interleukin-2. Not only are the receptors for these on the cell surface, but they are also heavily involved in the wound healing process, with measurable downstream effects [35,36]. Different multiscale tools to recognize different cell surface characteristics could potentially have applications in cancer detection, or treatments for arthritis and sickle cell anemia.

4.3 Geometric Considerations

As mentioned previously, it is important to consider geometric interactions of the components involved in the DNA origami tool itself in order to ensure consistent results. Once that framework has been established, the effect of different arrangements of peptide clusters on cellular response should be investigated as well. Geometric optimization will be essential to the efficacy of the system.

4.4 Conclusion

Throughout this work, the idea of using DNA origami to bridge the scale gap between cellular chemical signaling and mechanotransduction has been presented. While there are many aspects of this project that still require tuning, the design of the DNA origami tool and the subsequent questions raised by the preliminary results have lain the groundwork for future investigations of this type. By taking advantage of the unique physical and chemical properties of DNA, particularly its ability to molecularly self-assemble into discrete structures with sites functionalized with molecular precision, we have shown that there is some effect on cellular behavior when the gap between mechanotransduction and chemical signaling is bridged by our multiscale DNA origami tool. Continuing with the concepts explored in this work has the potential to change the way we understand cellular communication, opening many new platforms for innovation in biomedical technology.

REFERENCES

[1] Feynman, R.P. (1960). “There’s Plenty of Room at the Bottom.” *Engr. And Sci.* 23(5): 22,36.

[2] Whitesides, G.M. and B. Grzybowski (2002). Self Assembly at All Scales. Science 295(5564): 2418, 2421.

[3] Li, H., Carter, J. D. & LaBean, T. H. Nanofabrication by DNA self-assembly. *Materials Today* 12, 24-32, doi:10.1016/s1369-7021(09)70157-9 (2009).

[4] Seeman, N. C. DNA in a material world. *Nature* 421, 427-431, doi:10.1038/nature01406 (2003).

[5] D. Chester, R. Kathard, J. Nortey, K. Nellenbach, A.C. Brown. Viscoelastic properties of microgel thin films control fibroblast modes of migration and pro-fibrotic responses. *Biomaterials*, 185 (May) (2018), pp. 371-382

[6] Wong, V. W., Longaker, M. T. & Gurtner, G. C. Soft tissue mechanotransduction in wound healing and fibrosis. *Semin Cell Dev Biol* 23, 981-986, doi:10.1016/j.semcdb.2012.09.010 (2012).

[7] Rothemund, P. W. K. Folding DNA to create nanoscale shapes and patterns. *Nature* 440, 297-302, doi:10.1038/nature04586 (2006).

[8] Dickerson R.E. Definitions and nomenclature of nucleic acid structure components. *Nucleic Acids Res.* 1989; 17:1797–1803.

[9] Lu X.J., Olson W.K. Resolving the discrepancies among nucleic acid conformational analyses. *J Mol Biol.* 1999 Jan 29;285(4):1563-75. doi: 10.1006/jmbi.1998.2390. PMID: 9917397.

[10] Sinden, Richard R (1994-01-15). *DNA structure and function* (1st ed.). Academic Press. p. 398. ISBN 0-12-645750-6.

[11] Seeman, N. C. Nucleic-Acid Junctions and Lattices. *J Theor Biol* 99, 237-247, doi: 10.1016/0022-5193(82)90002-9 (1982).

[12] Xiaojun Li, Xiaoping Yang, Jing Qi, and Nadrian C. Seeman. *J. Am. Chem. Soc.* 1996 118 (26), 6131-6140. doi: 10.1021/ja960162o

[13] Pedersen, Ronnie & Marchi, Alexandria & Majikes, Jacob & Nash, Jessica & Estrich, Nicole & Courson, David & Hall, Carol & Craig, Stephen & Labean, Thomas. (2014). Properties of DNA. 10.1007/978-3-642-31107-9_10.

[14] Linko V, Dietz H. The enabled state of DNA nanotechnology. *Curr Opin Biotechnol*. 2013 Aug;24(4):555-61. doi: 10.1016/j.copbio.2013.02.001. Epub 2013 Apr 6. PMID: 23566376.

[15] Li, H. Y., LaBean, T. H. & Leong, K. W. Nucleic acid-based nanoengineering: novel structures for biomedical applications. *Interface Focus* 1, 702-724, doi:10.1098/rsfs.2011.0040 (2011).

[16] Nelson, David L.; Cox, Michael M. (2005), *Principles of Biochemistry* (4th ed.), New York: W. H. Freeman, ISBN 0-7167-4339-6

[17] Gupta A, Mishra A, Puri N. Peptide nucleic acids: Advanced tools for biomedical applications. *J Biotechnol.* 2017 Oct 10;259:148-159. doi: 10.1016/j.jbiotec.2017.07.026. Epub 2017 Jul 29. PMID: 28764969; PMCID: PMC7114329.

[18] Peter E. Nielsen, Michael Egholm, and Ole Buchardt. Peptide nucleic acid (PNA). A DNA mimic with a peptide backbone. *Chemistry* 1994 5 (1), 3-7. doi: 10.1021/bc00025a001.

[19] Li L, Klim JR, Derda R, Courtney AH, Kiessling LL. Spatial control of cell fate using synthetic surfaces to potentiate TGF-β signaling. *Proceedings of the National Academy of Sciences.* 2011;108(29):11745–11750. doi:10.1073/pnas.1101454108.

[20] Nguyen TT, Mobashery S, Chang M. Roles of Matrix Metalloproteinases in Cutaneous Wound Healing. *Wound Healing - New insights into Ancient Challenges*. 2016. doi:10.5772/64611

[21] Mihalko, E. P. & Brown, A. C. Material Strategies for Modulating Epithelial to Mesenchymal Transitions. *ACS Biomat. Sci. & Engr*, doi:10.1021/acsbiomaterials.6b00751 (2017).

[22] Wipff, P.-J., Rifkin, D. B., Meister, J.-J. & Hinz, B. Myofibroblast contraction activates latent TGF-β from the extracellular matrix. *J. Cell Bio.* 179, 1311-1323, doi:10.1083/jcb.200704042 (2007).

[23] Wrana JL, Attisano L, Wieser R, Ventura F, Massagué J. Mechanism of activation of the TGF-beta receptor. *Nature.* 1994 Aug 4;370(6488):341-7. doi: 10.1038/370341a0. PMID: 8047140.

[24] Pedersen, R. O., Loboa, E. G. & LaBean, T. H. Sensitization of Transforming Growth Factor-β Signaling by Multiple Peptides Patterned on DNA Nanostructures. *Biomacromolecules* 14, 4157- 4160, doi:10.1021/bm4011722 (2013).

[25] Chaudhuri, O. Viscoelastic hydrogels for 3D cell culture. *Biomaterials Science* 5, 1480-1490, doi:10.1039/c7bm00261k (2017).

[26] Bauer, A. et al. Hydrogel substrate stress-relaxation regulates the spreading and proliferation of mouse myoblasts. *Acta Biomater* 62, 82-90, doi:10.1016/j.actbio.2017.08.041 (2017).

[27] Bachman, H. et al. Ultrasoft, highly deformable microgels. *Soft Matter* 11, 2018-2028, doi:10.1039/c5sm00047e (2015).

[28] Brown, A. C. et al. Ultrasoft microgels displaying emergent platelet-like behaviours. *Nat*

Mater 13, 1108-1114, doi:10.1038/nmat4066 (2014).

[29] Kim, J., Park, Y., Brown, A. C. & Lyon, L. A. Direct observation of ligand-induced receptor dimerization with a bioresponsive hydrogel. *RSC Adv*. 4, 65173-65175, doi:10.1039/c4ra13251c (2014).

[30] Serpe, M. J., Jones, C. D. & Lyon, L. A. Layer-by-Layer Deposition of Thermoresponsive Microgel Thin Films. *Langmuir* 19, 8759-8764, doi:10.1021/la034391h (2003).

[31] South, A. B., Whitmire, R. E., Garcia, A. J. & Lyon, L. A. Centrifugal deposition of microgels for the rapid assembly of nonfouling thin films. *ACS Appl Mater Interfaces* 1, 2747-2754, doi:10.1021/am9005435 (2009).

[32] Marchi Alexandria N, Saaem I, Vogen B, Brown S, and LaBean T. Towards larger DNA origami. *Nano Letters* 2014 14 (10), 5740-5747. DOI: 10.1021/nl502626s

[33] McDavid A, Dennis L, Danaher P, Finak G, Krouse M, Wang A, et al. (2014) Modeling Bi-modality Improves Characterization of Cell Cycle on Gene Expression in Single Cells. *PLoS Comput Biol* 10(7): e1003696. https://doi.org/10.1371/journal.pcbi.1003696

[34] Jungmann R., Steinhauer C., Scheible M., Kuzyk A., Tinnefeld P., Simmel F.C. Single-Molecule Kinetics and Super-Resolution Microscopy by Fluorescence Imaging of Transient Binding on DNA Origami. *Nano Lett*. 2010;10:4756–4761. doi: 10.1021/nl103427w.

[35] Dao DT, Anez-Bustillos L, Adam RM, Puder M, Bielenberg DR. Heparin-Binding Epidermal Growth Factor-Like Growth Factor as a Critical Mediator of Tissue Repair and Regeneration. *Am J Pathol.* 2018;188(11):2446-2456. doi:10.1016/j.ajpath.2018.07.016

[36] Popescu M, Bogdan C, Pintea A, Rugină D, Ionescu C. Antiangiogenic cytokines as

potential new therapeutic targets for resveratrol in diabetic retinopathy. *Drug Des Devel Ther.* 2018;12:1985-1996. Published 2018 Jul 3. doi:10.2147/DDDT.S156941

APPENDICES

APPENDIX A: FULL STAPLE STRAND LIST FOR DNA ORIGAMI RECTANGLE

From Rothemund, P. W. K. Folding DNA to create nanoscale shapes and patterns. Nature 440, 297-302, doi:10.1038/nature04586 (2006).

Name	Start	End	Sequence
t-5r2f	1[32]	3[31]	TGAGTTTCAAAGGAACAACTAAAGATCTCCAA
t-5r4f	3[32]	5[31]	AAAAAAGGCTTTTGCGGGATCGTCGGGTAGCA
t-5r6f	5[32]	7[31]	ACGGCTACAAGTACAACGGAGATTCGCGACCT
t-5r8f	7[32]	9[31]	GCTCCATGACGTAACAAAGCTGCTACACCAGA
t-5r10f	9[32]	11[31]	ACGAGTAGATCAGTTGAGATTTAGCGCCAAAA
t-5r12f	11[32]	13[31]	GGAATTACCATTGAATCCCCCTCACCATAAAT
t-5r14f	13[32]	15[31]	CAAAAATCATTGCTCCTTTTGATAATTGCTGA
t-5r16f	15[32]	17[31]	ATATAATGGGGGCGCGAGCTGAAATTAACATC
t-5r18f	17[32]	19[31]	CAATAAATAAATGCAATGCCTGAGAAGGCCGG
t-5r20f	19[32]	21[31]	AGACAGTCTCATATGTACCCCGGTTTGTATAA
t-5r22f	21[32]	23[31]	GCAAATATGATTCTCCGTGGGAACCGTTGGTG
t-5r24f	23[32]	25[31]	TAGATGGGGTGCGGGCCTCTTCGCGCAAGGCG
t-5r26f	25[32]	27[31]	ATTAAGTTTTCCACACAACATACGCCTAATGA
t-5r28f	27[32]	29[31]	GTGAGCTAGCCCTTCACCGCCTGGGGTTTGCC
t-5r4e	4[47]	2[48]	AAAGGCCGCTCCAAAAGGAGCCTTAGCGGAGT
t-5r6e	6[47]	4[48]	GCGAAACAAGAGGCTTTGAGGACTAGGGAGTT
t-5r8e	8[47]	6[48]	CCAAATCATTACTTAGCCGGAACGTACCAAGC
t-5r10e	10[47]	8[48]	AAAGATTCTAAATTGGGCTTGAGATTCATTAC
t-5r12e	12[47]	10[48]	TAAATATTGAGGCATAGTAAGAGCACAGGTAG
t-5r14e	14[47]	12[48]	TACCTTTAAGGTCTTTACCCTGACAATCGTCA
t-5r16e	16[47]	14[48]	TTTCATTTCTGTAGCTCAACATGTTTAGAGAG
t-5r18e	18[47]	16[48]	TATATTTTCATACAGGCAAGGCAAAGCTATAT

t-5r20e	20[47]	18[48]	CATGTCAAAAATCACCATCAATATAACCCTCA
t-5r22e	22[47]	20[48]	ACCCGTCGTTAAATTGTAAACGTTAAAACTAG
t-5r24e	24[47]	22[48]	GGCGATCGCGCATCGTAACCGTGCGAGTAACA
t-5r26e	26[47]	24[48]	GCTCACAAGGGTAACGCCAGGGTTTTGGGAAG
t-5r28e	28[47]	26[48]	AGCTGATTACTCACATTAATTGCGTGTTATCC
t-5r30e	30[47]	28[48]	TATCAGGGCGAAAATCCTGTTTGACGGGCAAC
t-3r2f	1[64]	3[63]	TGTAGCATAACTTTCAACAGTTTCTAATTGTA
t-3r4f	3[64]	5[63]	TCGGTTTAGGTCGCTGAGGCTTGCAAAGACTT
t-3r6f	5[64]	7[63]	TTTCATGATGACCCCCAGCGATTAAGGCGCAG
t-3r8f	7[64]	9[63]	ACGGTCAATGACAAGAACCGGATATGGTTTAA
t-3r10f	9[64]	11[63]	TTTCAACTACGGAACAACATTATTAACACTAT
t-3r12f	11[64]	13[63]	CATAACCCGCGTCCAATACTGCGGTATTATAG
t-3r14f	13[64]	15[63]	TCAGAAGCCTCCAACAGGTCAGGATTTAAATA
t-3r16f	15[64]	17[63]	TGCAACTAGGTCAATAACCTGTTTAGAATTAG
t-3r18f	17[64]	19[63]	CAAAATTAGGATAAAAATTTTTAGGATATTCA
t-3r20f	19[64]	21[63]	ACCGTTCTGATGAACGGTAATCGTAATATTTT
t-3r22f	21[64]	23[63]	GTTAAAATAACATTAAATGTGAGCATCTGCCA
t-3r24f	23[64]	25[63]	GTTTGAGGTCAGGCTGCGCAACTGTTCCCAGT
t-3r26f	25[64]	27[63]	CACGACGTGTTTCCTGTGTGAAATTTGCGCTC
t-3r28f	27[64]	29[63]	ACTGCCCGCTTTTCACCAGTGAGATGGTGGTT
t-3r4e	4[79]	2[80]	ATATATTCTCAGCTTGCTTTCGAGTGGGATTT
t-3r6e	6[79]	4[80]	CTCATCTTGGAAGTTTCCATTAAACATAACCG
t-3r8e	8[79]	6[80]	AGTAATCTTCATAAGGGAACCGAACTAAAACA
t-3r10e	10[79]	8[80]	ACGAACTATTAATCATTGTGAATTTCATCAAG
t-3r12e	12[79]	10[80]	ACTGGATATCGTTTACCAGACGACTTAATAAA
t-3r14e	14[79]	12[80]	GAAGCAAAAAAGCGGATTGCATCAATGTTTAG

t-3r16e	16[79]	14[80]	TCGCAAATAAGTACGGTGTCTGGACCAGACCG
t-3r18e	18[79]	16[80]	CAACGCAAAGCAATAAAGCCTCAGGATACATT
t-3r20e	20[79]	18[80]	AGAGAATCAGCTGATAAATTAATGCTTTATTT
t-3r22e	22[79]	20[80]	CTTTCATCTCGCATTAAATTTTTGAGCAAACA
t-3r24e	24[79]	22[80]	TTCGCCATGGACGACGACAGTATCGTAGCCAG
t-3r26e	26[79]	24[80]	TCATAGCTTGTAAAACGACGGCCAAAGCGCCA
t-3r28e	28[79]	26[80]	TGGTTTTTCTTTCCAGTCGGGAAAAATCATGG
t-3r30e	30[79]	28[80]	TGGACTCCGGCAAAATCCCTTATACGCCAGGG
t-1r2f	1[96]	3[95]	CGTAACGAAAATGAATTTTCTGTAGTGAATTT
t-1r4f	3[96]	5[95]	CTTAAACAACAACCATCGCCCACGCGGGTAAA
t-1r6f	5[96]	7[95]	ATACGTAAGAGGCAAAAGAATACACTGACCAA
t-1r8f	7[96]	9[95]	CTTTGAAAATAGGCTGGCTGACCTACCTTATG
t-1r10f	9[96]	11[95]	CGATTTTAGGAAGAAAAATCTACGGATAAAAA
t-1r12f	11[96]	13[95]	CCAAAATAAGGGGGTAATAGTAAAAAAAGATT
t-1r14f	13[96]	15[95]	AAGAGGAACGAGCTTCAAAGCGAAAGTTTCAT
t-1r16f	15[96]	17[95]	TCCATATATTTAGTTTGACCATTAAGCATAAA
t-1r18f	17[96]	19[95]	GCTAAATCCTTTTGCGGGAGAAGCCCGGAGAG
t-1r20f	19[96]	21[95]	GGTAGCTATTGCCTGAGAGTCTGGTTAAATCA
t-1r22f	21[96]	23[95]	GCTCATTTCGCGTCTGGCCTTCCTGGCCTCAG
t-1r24f	23[96]	25[95]	GAAGATCGTGCCGGAAACCAGGCAGTGCCAAG
t-1r26f	25[96]	27[95]	CTTGCATGCCGAGCTCGAATTCGTCCTGTCGT
t-1r28f	27[96]	29[95]	GCCAGCTGCGGTTTGCGTATTGGGAATCAAAA
t-1r2e	2[111]	1[127]	ACGTTAGTTCTAAAGTTTTGTCGTGATACAGG
t-1r4e	4[111]	3[127]	CAATGACAGCTTGATACCGATAGTCTCCCTCA
t-1r6e	6[111]	5[127]	AAACGAAATGCCACTACGAAGGCAGCCAGCAA
t-1r8e	8[111]	7[127]	CCAGGCGCGAGGACAGATGAACGGGTAGAAAA

t-1r10e	10[111]	9[127]	GGACGTTGAGAACTGGCTCATTATGCGCTAAT
t-1r12e	12[111]	11[127]	TTTGCCAGGCGAGAGGCTTTTGCAATCCTGAA
t-1r14e	14[111]	13[127]	TTTTAATTGCCCGAAAGACTTCAACAAGAACG
t-1r16e	16[111]	15[127]	CGAGTAGAACAGTTGATTCCCAATATTTAGGC
t-1r18e	18[111]	17[127]	CTGTAATAGGTTGTACCAAAAACACAAATATA
t-1r20e	20[111]	19[127]	TCAGGTCATTTTTGAGAGATCTACCCTTGCTT
t-1r22e	22[111]	21[127]	AAATAATTTTTAACCAATAGGAACAACAGTAC
t-1r24e	24[111]	23[127]	GCTTCTGGCACTCCAGCCAGCTTTACATTATC
t-1r26e	26[111]	25[127]	CCCGGGTACCTGCAGGTCGACTCTCAAATATC
t-1r28e	28[111]	27[127]	GGGAGAGGCATTAATGAATCGGCCACCTGAAA
t-1r30e	30[111]	29[127]	AGTTTGGACGAGATAGGGTTGAGTGTAATAAC
t1r2f	1[128]	2[112]	AGTGTACTATACATGGCTTTTGATCTTTCCAG
t1r4f	3[128]	4[112]	GAGCCGCCCCACCACCGGAACCGCTGCGCCGA
t1r6f	5[128]	6[112]	AATCACCACCATTTGGGAATTAGACCAACCTA
t1r8f	7[128]	8[112]	TACATACACAGTATGTTAGCAAACTGTACAGA
t1r10f	9[128]	10[112]	ATCAGAGAGTCAGAGGGTAATTGAACCAGTCA
t1r12f	11[128]	12[112]	TCTTACCAACCCAGCTACAATTTTAAAGAAGT
t1r14f	13[128]	14[112]	GGTATTAATCTTTCCTTATCATTCATATCGCG
t1r16f	15[128]	16[112]	AGAGGCATACAACGCCAACATGTATCTGCGAA
t1r18f	17[128]	18[112]	TTTTAGTTCGCGAGAAAACTTTTTTTATGACC
t1r20f	19[128]	20[112]	CTGTAAATATATGTGAGTGAATAAAAAGGCTA
t1r22f	21[128]	22[112]	CTTTTACACAGATGAATATACAGTGCCATCAA
t1r24f	23[128]	24[112]	ATTTTGCGTTTAAAAGTTTGAGTACCGGCACC
t1r26f	25[128]	26[112]	AAACCCTCTCACCTTGCTGAACCTAGAGGATC

t1r28f	27[128]	28[112]	GCGTAAGAAGATAGAACCCTTCTGAACGCGCG
t1r30f	29[128]	30[112]	ATCACTTGAATACTTCTTTGATTAGTTGTTCC
t1r4e	4[143]	2[144]	AACCAGAGACCCTCAGAACCGCCACGTTCCAG
t1r6e	6[143]	4[144]	GACTTGAGGTAGCACCATTACCATATCACCGG
t1r8e	8[143]	6[144]	TTATTACGTAAAGGTGGCAACATACCGTCACC
t1r10e	10[143]	8[144]	TGAACAAAGATAACCCACAAGAATAAGACTCC
t1r12e	12[143]	10[144]	TATTTTGCACGCTAACGAGCGTCTGAACACCC
t1r14e	14[143]	12[144]	ATCGGCTGACCAAGTACCGCACTCTTAGTTGC
t1r16e	16[143]	14[144]	CATATTTATTTCGAGCCAGTAATAAATCAATA
t1r18e	18[143]	16[144]	ACAAAGAAAATTTCATCTTCTGACAGAATCGC
t1r20e	20[143]	18[144]	AAATCAATCGTCGCTATTAATTAAATCGCAAG
t1r22e	22[143]	20[144]	TTTAACGTTCGGGAGAAACAATAACAGTACAT
t1r24e	24[143]	22[144]	TTATTAATGAACAAAGAAACCACCTTTTCAGG
t1r26e	26[143]	24[144]	CTAAAGCAAATCAATATCTGGTCACCCGAACG
t1r28e	28[143]	26[144]	GCCAACAGATACGTGGCACAGACATGAAAAAT
t1r30e	30[143]	28[144]	GTTGTAGCCCTGAGTAGAAGAACTACATTCTG
t3r2f	1[160]	3[159]	TGCCTTGACAGTCTCTGAATTTACCCCTCAGA
t3r4f	3[160]	5[159]	GCCACCACTCTTTTCATAATCAAATAGCAAGG
t3r6f	5[160]	7[159]	CCGGAAACTAAAGGTGAATTATCATAAAAGAA
t3r8f	7[160]	9[159]	ACGCAAAGAAGAACTGGCATGATTTGAGTTAA
t3r10f	9[160]	11[159]	GCCCAATAGACGGGAGAATTAACTTTCCAGAG
t3r12f	11[160]	13[159]	CCTAATTTAAGCCTTAAATCAAGAATCGAGAA
t3r14f	13[160]	15[159]	CAAGCAAGCGAGCATGTAGAAACCAGAGAATA
t3r16f	15[160]	17[159]	TAAAGTACCAGTAGGGCTTAATTGCTAAATTT
t3r18f	17[160]	19[159]	AATGGTTTTGCTGATGCAAATCCATTTTCCCT
t3r20f	19[160]	21[159]	TAGAATCCCCTTTTTTAATGGAAACGGATTCG

t3r22f	21[160]	23[159]	CCTGATTGAAAGAAATTGCGTAGAAGAAGGAG
t3r24f	23[160]	25[159]	CGGAATTACGTATTAAATCCTTTGGTTGGCAA
t3r26f	25[160]	27[159]	ATCAACAGGAGAGCCAGCAGCAAAATATTTTT
t3r28f	27[160]	29[159]	GAATGGCTACCAGTAATAAAAGGGCAAACTAT
t3r4e	4[175]	2[176]	GTTTGCCACCTCAGAGCCGCCACCGCCAGAAT
t3r6e	6[175]	4[176]	TTATTCATGTCACCAATGAAACCATTATTAGC
t3r8e	8[175]	6[176]	ATACCCAAACACCACGGAATAAGTGACGGAAA
t3r10e	10[175]	8[176]	GCGCATTAATAAGAGCAAGAAACAATAACGGA
t3r12e	12[175]	10[176]	AGGTTTTGGCCAGTTACAAAATAAACAGGGAA
t3r14e	14[175]	12[176]	CTAATTTACCGTTTTTATTTTCATCTTGCGGG
t3r16e	16[175]	14[176]	ACGCTCAACGACAAAAGGTAAAGTATCCCATC
t3r18e	18[175]	16[176]	TATGTAAAGAAATACCGACCGTGTTAAAGCCA
t3r20e	20[175]	18[176]	TTGAATTATTGAAAACATAGCGATTATAACTA
t3r22e	22[175]	20[176]	ACAGAAATCTTTGAATACCAAGTTAATTTCAT
t3r24e	24[175]	22[176]	CGACAACTTCATCATATTCCTGATCACGTAAA
t3r26e	26[175]	24[176]	GCCACGCTTTGAAAGGAATTGAGGAAACAATT
t3r28e	28[175]	26[176]	GTCACACGATTAGTCTTTAATGCGGCAACAGT
t3r30e	30[175]	28[176]	GTAAAAGACTGGTAATATCCAGAAATTCACCA
t5r2f	1[192]	3[191]	AATGCCCCATAAATCCTCATTAAAAGAACCAC
t5r4f	3[192]	5[191]	CACCAGAGTTCGGTCATAGCCCCCTCGATAGC
t5r6f	5[192]	7[191]	AGCACCGTAGGGAAGGTAAATATTTTATTTTG
t5r8f	7[192]	9[191]	TCACAATCCCGAGGAAACGCAATAATGAAATA
t5r10f	9[192]	11[191]	GCAATAGCAGAGAATAACATAAAAACAGCCAT
t5r12f	11[192]	13[191]	ATTATTTATTAGCGAACCTCCCGACGTAGGAA
t5r14f	13[192]	15[191]	TCATTACCGAACAAGAAAAATAATAATTCTGT
t5r16f	15[192]	17[191]	CCAGACGACAAATTCTTACCAGTAGATAAATA

t5r18f	17[192]	19[191]	AGGCGTTAGGCTTAGGTTGGGTTAAGCTTAGA
t5r20f	19[192]	21[191]	TTAAGACGATTAATTACATTTAACACAAAATC
t5r22f	21[192]	23[191]	GCGCAGAGATATCAAAATTATTTGTATCAGAT
t5r24f	23[192]	25[191]	GATGGCAAAAGTATTAGACTTTACAAGGTTAT
t5r26f	25[192]	27[191]	CTAAAATAAGTATTAACACCGCCTCGAACTGA
t5r28f	27[192]	29[191]	TAGCCCTATTATTTACATTGGCAGCAATATTA
t5r4e	4[207]	2[208]	TCGGCATTCCGCCGCCAGCATTGATGATATTC
t5r6e	6[207]	4[208]	ATTGAGGGAATCAGTAGCGACAGACGTTTTCA
t5r8e	8[207]	6[208]	GAAGGAAAAATAGAAAATTCATATTTCAACCG
t5r10e	10[207]	8[208]	CTTTACAGTATCTTACCGAAGCCCAGTTACCA
t5r12e	12[207]	10[208]	GAGGCGTTTCCCAATCCAAATAAGATAGCAGC
t5r14e	14[207]	12[208]	TAAGTCCTGCGCCCAATAGCAAGCAAGAACGC
t5r16e	16[207]	14[208]	GCGTTATACGACAATAAACAACATACAATAGA
t5r18e	18[207]	16[208]	TAACCTCCAATAAGAATAAACACCTATCATAT
t5r20e	20[207]	18[208]	AAAACAAACTGAGAAGAGTCAATATACCTTTT
t5r22e	22[207]	20[208]	AACCTACCGCGAATTATTCATTTCACATCAAG
t5r24e	24[207]	22[208]	GGATTTAGTTCATCAATATAATCCAGGGTTAG
t5r26e	26[207]	24[208]	AGGCGGTCTCTTTAGGAGCACTAAACATTTGA
t5r28e	28[207]	26[208]	GAAATGGAAAACATCGCCATTAAACAGAGGTG
t5r30e	30[207]	28[208]	AGAAGTGTCATTGCAACAGGAAAAAATCGTCT
t-5r0g	0[47]	1[31]	CTCAGAGCCACCACCCTCATTTTCCGTAACAC
t-3r0g	0[79]	1[63]	CCCTCAGAACCGCCACCCTCAGAAACAACGCC
t-1r0g	0[111]	1[95]	TATCACCGTACTCAGGAGGTTTAGATAGTTAG
t1r0g	0[143]	0[112]	AGGGTTGATATAAGTATAGCCCGGAATAGGTG
t3r0g	0[175]	1[159]	TGCTCAGTACCAGGCGGATAAGTGGGGGTCAG
t5r0g	0[207]	1[191]	CCTCAAGAGAAGGATTAGGATTAGAAACAGTT
t-5r2e	2[47]	0[48]	GAGAATAGGTCACCAGTACAAACTCCGCCACC
t-3r2e	2[79]	0[80]	TGCTAAACTCCACAGACAGCCCTCTACCGCCA

t1r2e	2[143]	0[144]	TAAGCGTCGGTAATAAGTTTTAACCCGTCGAG
t3r2e	2[175]	0[176]	GGAAAGCGGTAACAGTGCCCGTATCGGGGTTT
t5r2e	2[207]	0[208]	ACAAACAACTGCCTATTTCGGAACCTGAGACT
t-5r32h	31[32]	30[48]	GTAAAGCACTAAATCGGAACCCTAAAACCGTC
t-3r32h	31[64]	30[80]	CCCCGATTTAGAGCTTGACGGGGAAAAGAACG
t-1r32h	31[96]	31[127]	GAACGTGGCGAGAAAGGAAGGGAATGCGCCGC
t1r32h	31[128]	30[144]	TACAGGGCGCGTACTATGGTTGCTAATTAACC
t3r32h	31[160]	30[176]	CACGTATAACGTGCTTTCCTCGTTGCCACCGA
t5r32h	31[192]	30[208]	AGCGGGAGCTAAACAGGAGGCCGAGAATCCTG
t-5r30f	29[32]	31[31]	CCAGCAGGCGATGGCCCACTACGTGAGGTGCC
t-3r30f	29[64]	31[63]	CCGAAATCAACGTCAAAGGGCGAAAAGGGAGC
t-1r30f	29[96]	31[95]	GAATAGCCACAAGAGTCCACTATTAAGCCGGC
t3r30f	29[160]	31[159]	CGGCCTTGGTCTGTCCATCACGCATTGACGAG
t5r30f	29[192]	31[191]	CCGCCAGCTTTTATAATCAGTGAGAGAATCAG
t-7r2i	2[15]	0[8]	AATAATAATTTTATAGGAACCCATGTACAGGGATAGCAAGCCCA
t-7r4e	4[15]	2[16]	CAGCGAAATTTTTTTTTTCACGTTGAAAGAATTGCG
t-7r6e	6[15]	4[16]	CGCCTGATTTTTGACAGCATCGGAACGAACCCTCAG
t-7r8e	8[15]	6[16]	GAATAAGGTTTTAAATTGTGTCGAAATCTGTATCAT
t-7r10e	10[15]	8[16]	CATTCAACTTTTCTTGCCCTGACGAGAACATTCAGT
t-7r12e	12[15]	10[16]	AAACAGTTTTTTTAATGCAGATACATAAGAATACCA
t-7r14e	14[15]	12[16]	TTTTTGCGTTTTCAGAAAACGAGAATGAAATGCTTT
t-7r16e	16[15]	14[16]	TCAATTCTTTTTGATGGCTTAGAGCTTAAGAGGTCA
t-7r18e	18[15]	16[16]	AGGTAAAGTTTTACTAATAGTAGTAGCAAGGTGGCA
t-7r20e	20[15]	18[16]	AGAAAAGCTTTTATTCAAAAGGGTGAGATAATGTGT
t-7r22e	22[15]	20[16]	GATTGACCTTTTCCCAAAAACAGGAAGATGATAATC

t-7r24e	24[15]	22[16]	CAGCTGGCTTTTGTAATGGGATAGGTCAAAACGGCG
t-7r26e	26[15]	24[16]	GCATAAAGTTTTGAAAGGGGGATGTGCTTATTACGC
t-7r28e	28[15]	26[16]	GAGTTGCATTTTTGTAAAGCCTGGGGTGAGCCGGAA
t-7r30e	30[15]	28[16]	ACCCAAATTTTTGCAAGCGGTCCACGCTCCCTGAGA
t-7r32e	31[4]	30[16]	TTTTCAAGTTTTTTGGGGTCGAACCATC
t7r0f	0[235]	1[223]	TTTTTGAAAGTATTAAGAGGCTATTATT
t7r2f	1[224]	3[223]	CTGAAACATTTTGTCAGACGATTGGCCTCAGGAGGT
t7r4f	3[224]	5[223]	TGAGGCAGTTTTGCGTCAGACTGTAGCGATCAAGTT
t7r6f	5[224]	7[223]	TGCCTTTATTTTAGACAAAAGGGCGACAGGTTTACC
t7r8f	7[224]	9[223]	AGCGCCAATTTTGCAGATAGCCGAACAATTTTTAAG
t7r10f	9[224]	11[223]	AAAAGTAATTTTAACGTCAAAAATGAAAAAACGATT
t7r12f	11[224]	13[223]	TTTTGTTTTTTTGCTTATCCGGTATTCTAAATCAGA
t7r14f	13[224]	15[223]	TATAGAAGTTTTACGCGCCTGTTTATCAGTTCAGCT
t7r16f	15[224]	17[223]	AATGCAGATTTTGAAAAAGCCTGTTTAGGGAATCAT
t7r18f	17[224]	19[223]	AATTACTATTTTCATAGGTCTGAGAGACGTGAATTT
t7r20f	19[224]	21[223]	ATCAAAATTTTTGAAGATGATGAAACAAAATTACCT
t7r22f	21[224]	23[223]	GAGCAAAATTTTACTTCTGAATAATGGATGATTGTT
t7r24f	23[224]	25[223]	TGGATTATTTTTGCCGTCAATAGATAATCAACTAAT
t7r26f	25[224]	27[223]	AGATTAGATTTTCCAGCAGAAGATAAAAAATACCGA
t7r28f	27[224]	29[223]	ACGAACCATTTTCTACATTTTGACGCTCACGCTCAT
t7r30j	29[224]	31[231]	GGAAATACTTTTCAGGAACGGTACGCCATTAAAGGGATTTTAGA

APPENDIX B: EXPLANATION OF REPLACEMENT STAPLE STRANDS

B.1 Site Justification and Alteration

Staple sites were chosen on the basis that, for both sides, some ought to be proximal to the center of the origami and some ought to be distal. On the O side, it was decided that this arrangement would provide adequate attachment, both in terms of structural stability.

In terms of the P side, it isn't known what spacing between sites is optimal for TGF-β sensitization. The work by Pedersen et al. featured a design in which peptide was clustered entirely at the center of the origami using biotinylated staples, avidin protein linkers, and biotinylated peptide [Pederson, Loboa et al.]. This project was designed to take that a step further and thus more sites, in a more complex arrangement, were chosen. Several sites remained clustered at the center of the origami, but four distal to the center were also included. This offers the opportunity for eventual studies into optimal spacing without having to alter the standing design of the origami.

The chosen sites – and sides – of the origami were based on work by Dr. Alexandra Marchi, which indicated that a certain side of Rothemund's rectangle, when not twist-corrected, would fall face down onto the substrate with slightly more frequency than the other side [Marchi et al.]. Thus, the O side was chosen as the one which tended to deposit downward.

By the nature of the rectangle design, staple strand "nicks" – the 5' end of one staple adjacent to the 3' end of the next staple – all were on the same side, the O side, of the origami. Therefore, functionalizing the O side was relatively trivial, as the handle falls on the 5' end: 5' sites were chosen, and those staples extended. The P side provided slightly more complications, as staples had to be cut in new locations and spliced together in others in order to have the 3' ends on the opposite side, the P side, of the origami. This is done by selecting a site on the other

side of the helix from the existing nicks and cutting the staple strand there, then splicing resulting staples with their adjacent neighbors. This results in non-functionalized "fractional" replacement staples, i.e. those which do not have the functional P* Anchor site but are necessary to maintain the structural integrity of the origami. The list of replacement strands, as well as their corresponding original Rothemund strands and an image of their location on the origami, follows.

The colored portions of the sequences are the handles of the staple extensions, i.e. the functional regions. Their complements in Anchor and P-PNA-Peptide sequences are listed in Appendix C, denoted by a different shade of the same color.

B.2 Replacement Staple Sequences and Diagram of Locations

Side O

O_Out1: 5'- TAC GAG TTG AGA ATC CTG AAT GCG--TT—
TTTCATGATGACCCCCAGCGATTAAGGCGCAG-3'

O_Out2: 5'- TAC GAG TTG AGA ATC CTG AAT GCG--TT—
CCGGAAACTAAAGGTGAATTATCATAAAAGAA -3'

O_Out3: 5'- TAC GAG TTG AGA ATC CTG AAT GCG--TT—
ACTGCCCGCTTTTCACCAGTGAGATGGTGGTT -3'

O_Out4: 5'- TAC GAG TTG AGA ATC CTG AAT GCG --TT—
GAATGGCTACCAGTAATAAAAGGGCAAACTAT -3'

Replacing: t-3r6f, t3r6f, t-3r28f, t3r28f

O_Cent1: 5'- TAC GAG TTG AGA ATC CTG AAT GCG--TT—
ACAAAGAAAATTTCATCTTCTGACAGAATCGC-3'

O_Cent2: 5’- TAC GAG TTG AGA ATC CTG AAT GCG--TT—

TTTTAGTTCGCGAGAAAACTTTTTTTATGACC-3’

O_Cent3: 5’- TAC GAG TTG AGA ATC CTG AAT GCG--TT—

CTGTAATAGGTTGTACCAAAAACACAAATATA-3’

O_Cent4: 5’- TAC GAG TTG AGA ATC CTG AAT GCG--TT—

CTGTAAATATATGTGAGTGAATAAAAAGGCTA-3’

Replacing: t1r18e, t1r18f, t-1r18e, t1r20f

Side P

P*_Cent1: 5’ AACATGTATCTGCGAACGAGTAGAACAGTTGA –TT- TGC AGT CAC CAA CGC 3’

P*_Cent2: 5’ AAAGCGAAAGTTTCATTCCATATATTTAGTTT-TT- TGC AGT CAC CAA CGC 3’

P*_Cent3: 5’ GACTTCAACAAGAACGGGTATTAATCTTTCCT –TT- TGC AGT CAC CAA CGC 3’

P*_Cent4: TATCATTCATATCGCGTTTTAATTGCCCGAAA-TT- TGC AGT CAC CAA CGC 3’

Fractional Staples:

P*_Cent1_Frac1: TTCCCAATATTTAGGCAGAGGCATACAACGCC

P*_Cent2_Frac1: AAGAGGAACGAGCTTC

P*_Cent2_Frac2: GACCATTAAGCATAAA

Replacing: t-1r14f, t-1r16f, t-1r14e, t1r14f, t-1r16e, & t1r16f

P*_Out1: 5’ TAGCAAACTGTACAGACCAGGCGCGAGGACAG-TT- TGC AGT CAC CAA CGC 3’

P*_Out2: 5’ GGTAAAGTATCCCATCCTAATTTACCGTTTTT-TT- TGC AGT CAC CAA CGC 3’

P*_Out3: 5’TTTGAGTACCGGCACCGCTTCTGGCACTCCAG-TT-TGC AGT CAC CAA CGC 3’

P*_Out4: 5’ CAACATGTTTAGAGAGTACCTTTAAGGTCTTT-TT- TGC AGT CAC CAA CGC 3’

Fractional Staples:

P*_Out1_Frac1: ATGAACGGGTAGAAAATACATACACAGTATGT

P*_Out2_Frac1: ATTTTCATCTTGCGGG

P*_Out2_Frac2: ACGCTCAACGACAAAA

P*_Out3_Frac1: CCAGCTTTACATTATCATTTTGCGTTTAAAAG

P*_Out4_Frac1: ACCCTGACAATCGTCA

P*_Out4_Frac2: TTTCATTTCTGTAGCT

Replacing: t-1r8e, t1r8f, t3r16e, t3r14e, t-1r24e, t1r24f, t-5r16e, & t-5r14e

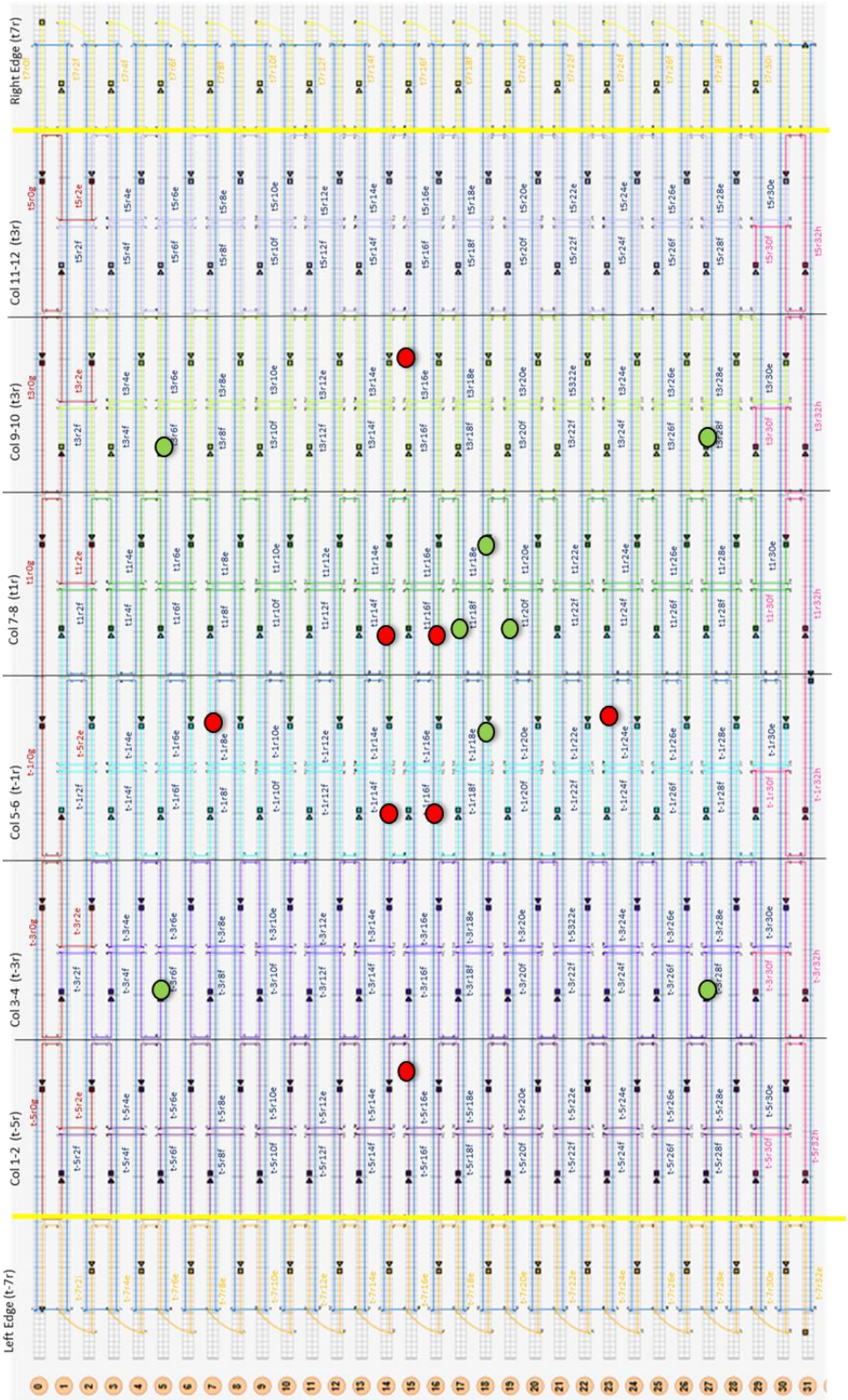

Figure B.1: A 2D model of the DNA origami structure showing all staple strands and replacement staple locations. P sites are red and should be visualized as extending through the page. O sites are green and extend up from the page.

APPENDIX C: ANCHOR, PROBE, AND PEPTIDE SEQUENCES

Complementary sequences are denoted by different shades of the same color. The complement of the O* Anchor can be found in the O Handle sequences listed in Appendix B.

P* Anchor
5'-NH_2-C_6-TTT TTA TGC AGT CAC CAA CGC -3'

P Probe
5'-Cy5-GCG TTG GTG ACT GCA TAA AAA-3'

PNA-Peptide
5'-LTGKNFPMFHRN-3'

P-PNA-Peptide
5'- LTGKNFPMFHRN -GCG TTG GTG ACT GCA-3'

O* Anchor
5'- CGC ATT CAG GAT TCT CAA CTC GTA TTTT -C_6-NH_2 -3'

APPENDIX D: CELL IMAGES AND SAMPLE ANALYSIS

D.1 Using ImageJ to Analyze Images

For the purposes of discussion, all of the included images are samples that have been coated with FN.

All images were collected on an EVOS fluorescent microscope which belongs to the laboratory of Professor Brown. Nuclei were stained with NucBlue for ease of live cell location while imaging; samples were imaged pre- and post-fixation; all images presented here are prior to fixation and were therefore captured while the samples were in 12 well plates. All of the presented images were captured at the 24 hour mark.

All images were analyzed using ImageJ software. The software parameters can be adjusted for capturing features of designated shape and size. However, even the most stringently selected search criteria will have exceptions, either those that cannot be captured through software or those which must be discarded. Therefore, the more complex cell shapes had to be traced "by hand" in the software, and some features misidentified as cells were removed from the data set after collation.

Example parameters, tracing, and identification of features correctly selected by the software follow, in addition to the image set used as representative data in this thesis.

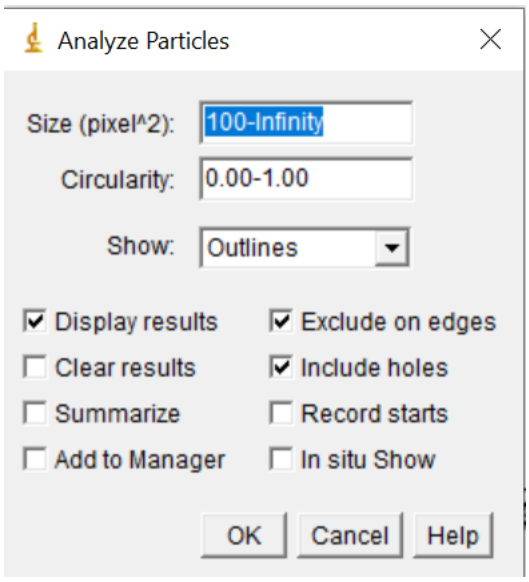

Figure D.1: Parameters used to select cells for analysis on ImageJ. Note the highlighted value: pixel size does not necessarily correspond directly to micrometers, the conversion must be determined from the scale of the original image.

The drop-down menu used in ImageJ to set search parameters for round cell analysis is shown in Figure D.1. The "size" option (highlighted) is the most important to determining which cells to initially select. If cells are too abnormal in shape, then instead of this search parameter, the free-hand tracing tool must be used instead of this parameter option set. However, even if objects in the image that are not cells are highlighted, the generated image of selected features is also labeled by number, so incorrect values can be discarded from the final data set. Figure B.2 shows an initial image, top left, (one not used in data analysis for this thesis), a processed image on the bottom left, and the generated column of values on the right. Object #17 (corresponding to the numbers in Column A and the label on the processed image) is not a cell and can be removed from the data set.

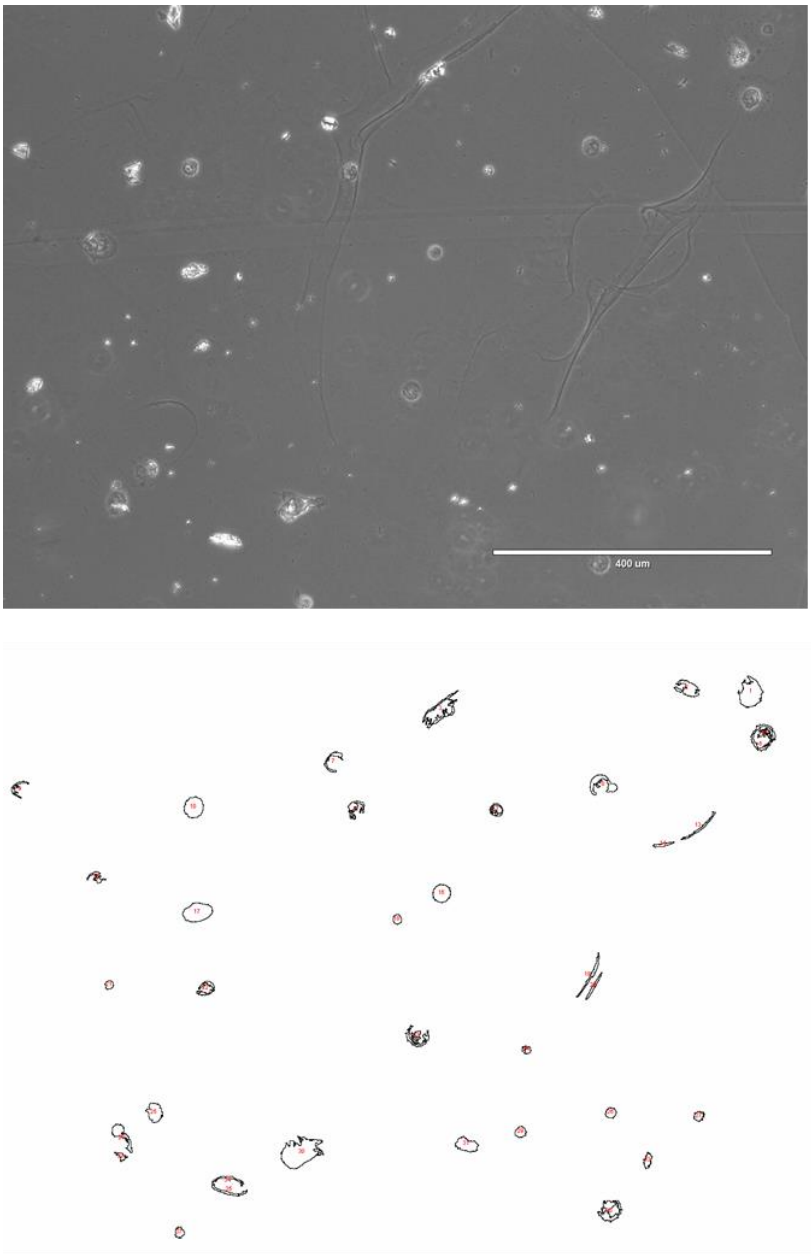

	A	B	C	D
1		Area	Perim.	Circ.
2	1	1163	204.492	0.349
3	2	514	190.593	0.178
4	3	454	486.382	0.024
5	4	186	157.823	0.094
6	5	132	149.238	0.074
7	6	143	122.51	0.12
8	7	187	154.409	0.099
9	8	514	212.25	0.143
10	9	132	149.095	0.075
11	10	766	111.882	0.769
12	11	263	218.836	0.069
13	12	135	156.309	0.069
14	13	166	166.108	0.076
15	14	111	78.426	0.227
16	15	152	133.338	0.107
17	16	605	104.368	0.698
18	17	1035	133.439	0.73
19	18	158	46.87	0.904
20	19	219	179.622	0.085
21	20	138	110.368	0.142
22	21	133	45.113	0.821
23	22	195	177.522	0.078
24	23	379	326.416	0.045
25	24	106	65.74	0.308
26	25	528	109.539	0.553
27	26	209	57.841	0.785
28	27	174	71.74	0.425
29	28	441	176.208	0.178
30	29	222	60.669	0.758
31	30	1929	353.487	0.194
32	31	545	117.095	0.499
33	32	103	70.083	0.264
34	33	195	83.882	0.348
35	34	127	137.539	0.084
36	35	187	148.61	0.106
37	36	529	284.718	0.082
38	37	180	59.841	0.632

Figure D.2: A sample of ImageJ analysis. The top left image is an unprocessed .tiff, the bottom left is the generated image after the search parameters have been engaged, and the right chart is the values generated from this search.

This process can be used in tandem with the hand tracing feature, which was necessary for images that were particularly representative of the bimodal distribution. The following images were used to generate the graph demonstrating the bimodal distribution, Figure 3.3.

D.2 Images Used for Representative Data Analysis

D.2.1 Samples without Fibronectin

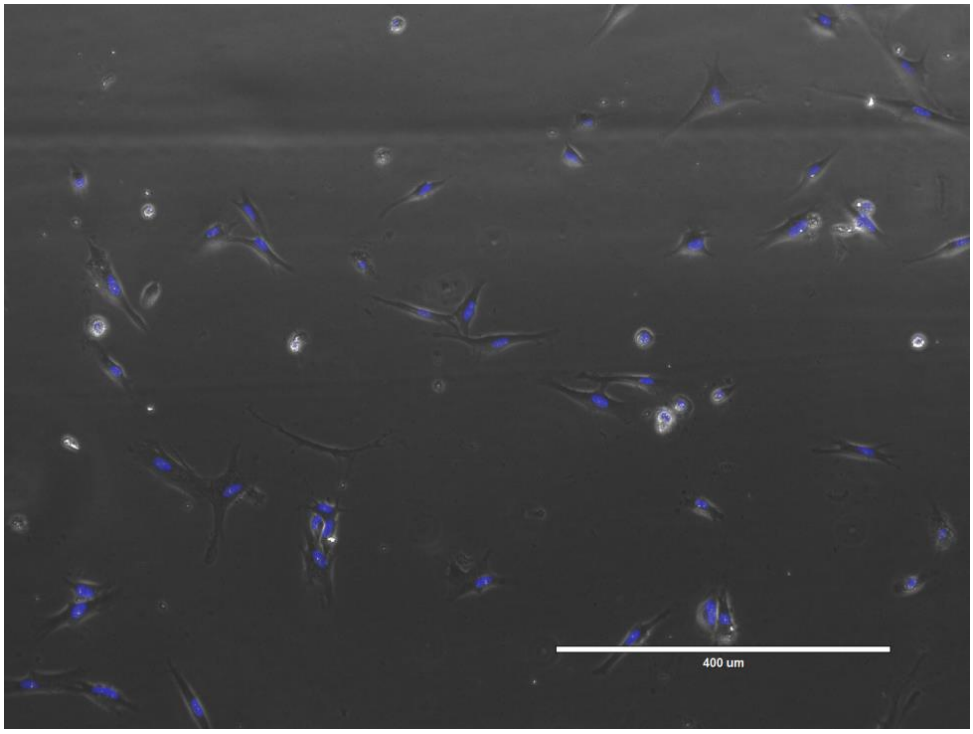

Figure D.3: HDFn cells on glass control substrate, not FN coated. Note that cells still spread, but many are circular. Live cells can be identified by blue-stained nuclei.

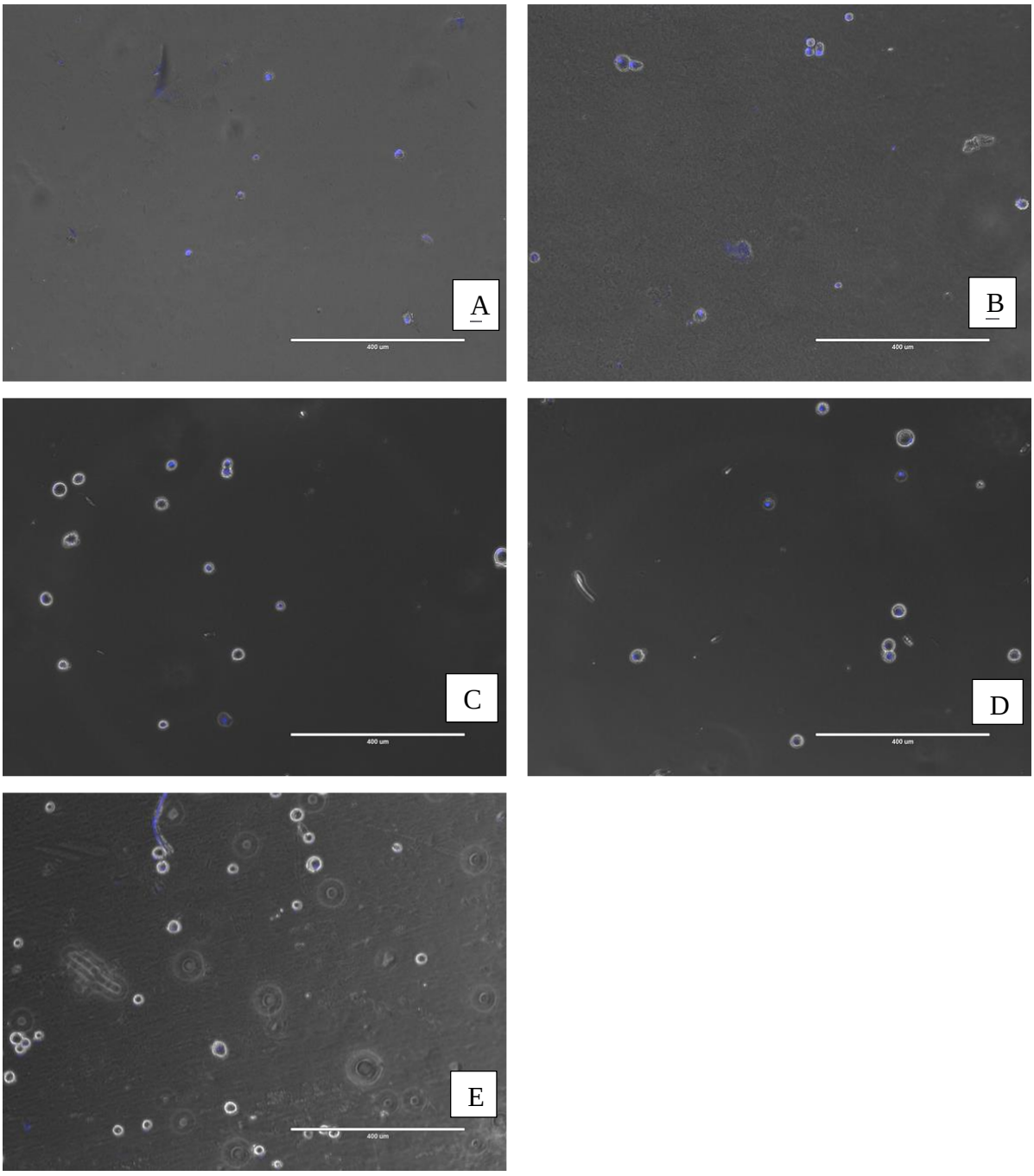

Figure D.4: Cells on 1% BIS crosslinked microgels. A) Unfunctionalized (microgel and cells), functionalized with B) P*+Pep, C) P*+Pep+TGF-B, D) Full Tool, E) Full Tool+TGF-B. All scale bars are 400 microns. There is little difference in area or circularity, and there are low cell counts between all images.

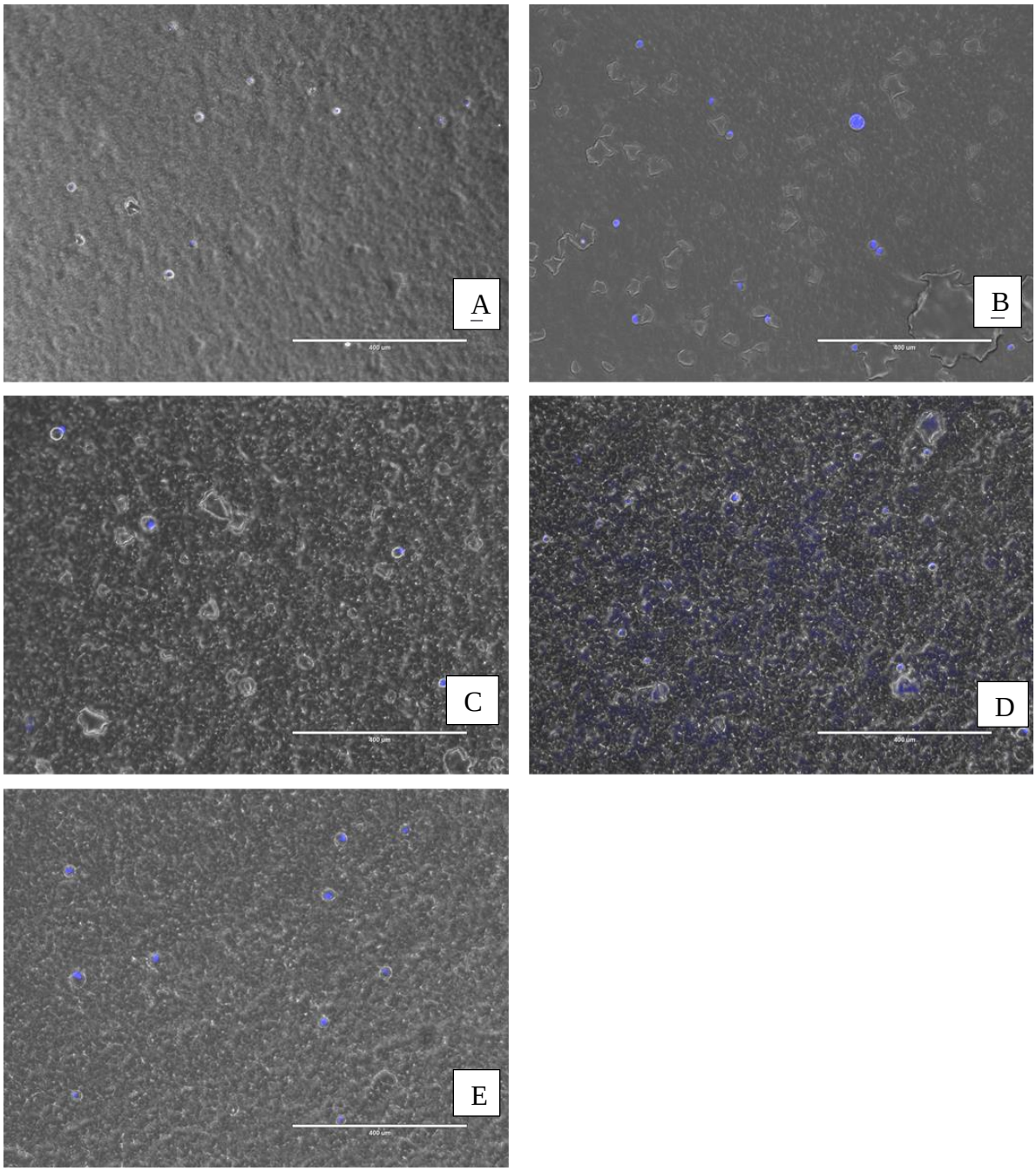

Figure D.5: Cells on 7% BIS crosslinked microgels. A) Unfunctionalized (microgel and cells), functionalized with B) P*+Pep, C) P*+Pep+TGF-B, D) Full Tool, E) Full Tool+TGF-B. All scale bars are 400 microns. Several cells in (A) may be dead, and overall adhesion and spreading is poor.

D.2.2 Samples with Fibronectin

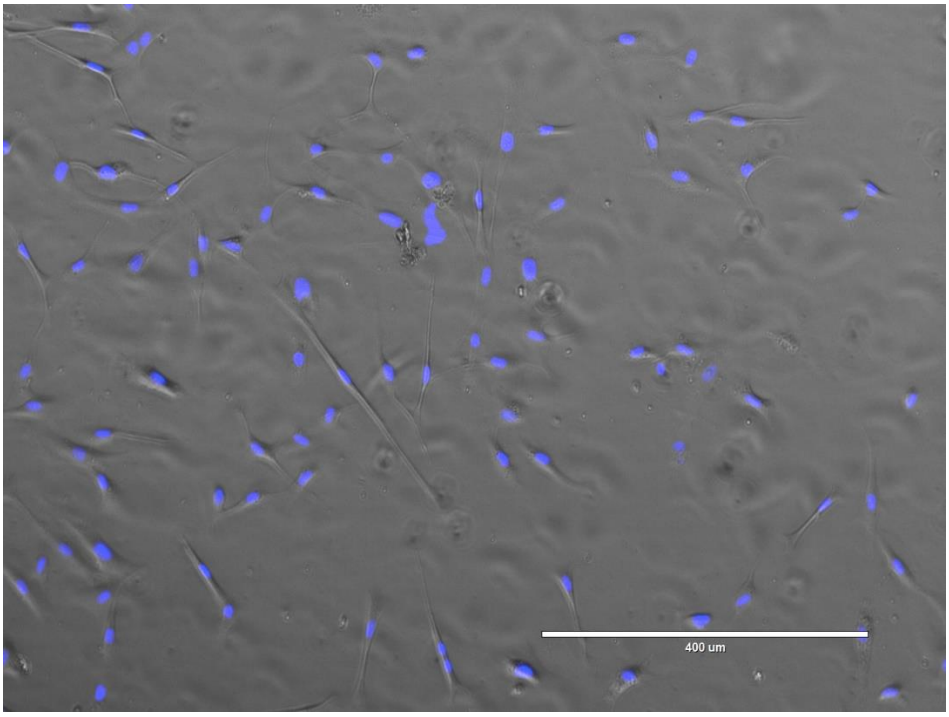

Figure D.6: HDFn cells on glass control substrate coated in FN. All cells have spread and are proliferating.

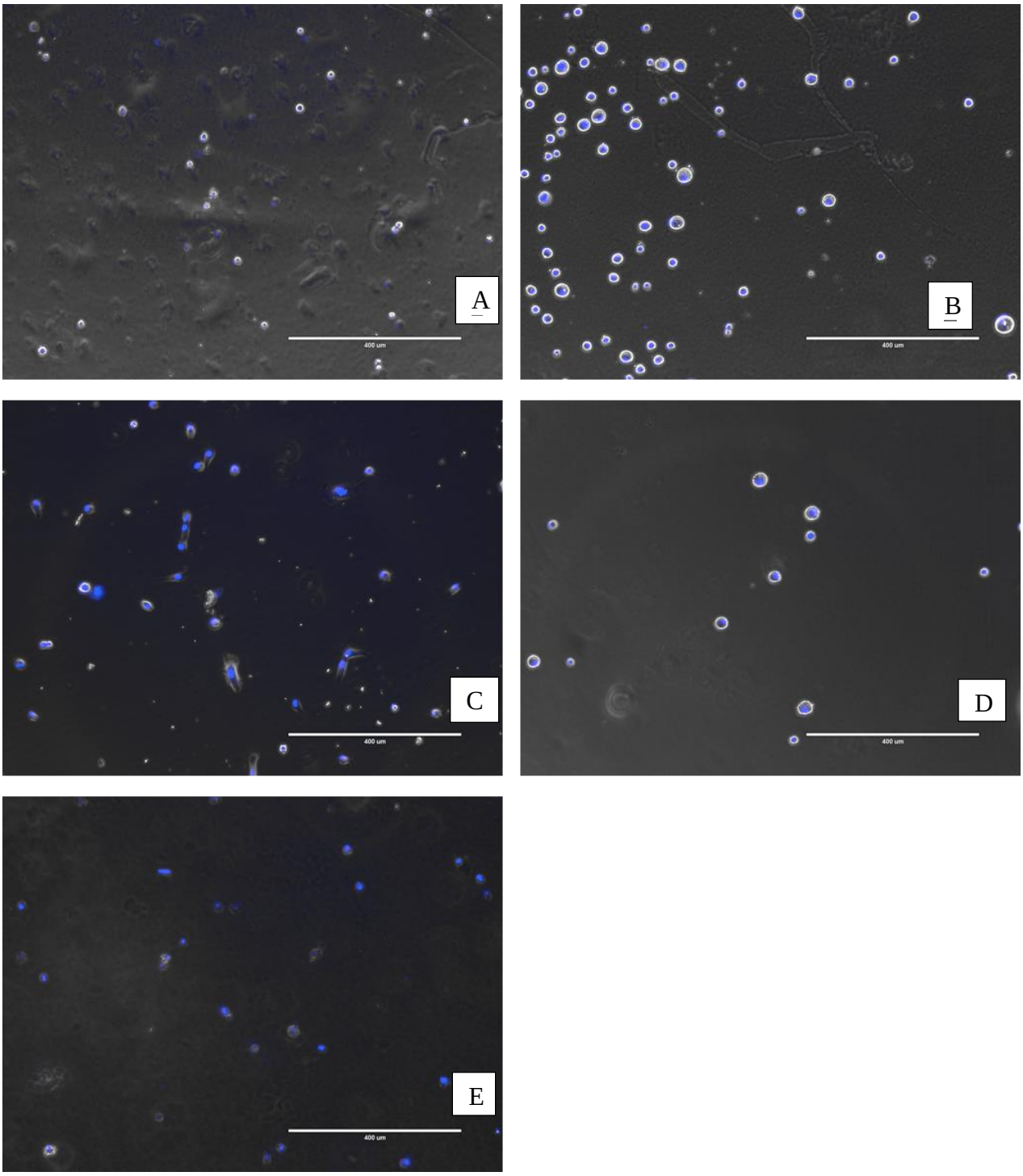

Figure D.7: Cells on 1% BIS crosslinked microgels. A) Unfunctionalized (microgel and cells), functionalized with B) P*+Pep, C) P*+Pep+TGF-B, D) Full Tool, E) Full Tool+TGF-B. All scale bars are 400 microns. Some spreading is seen, and cell count is improved.

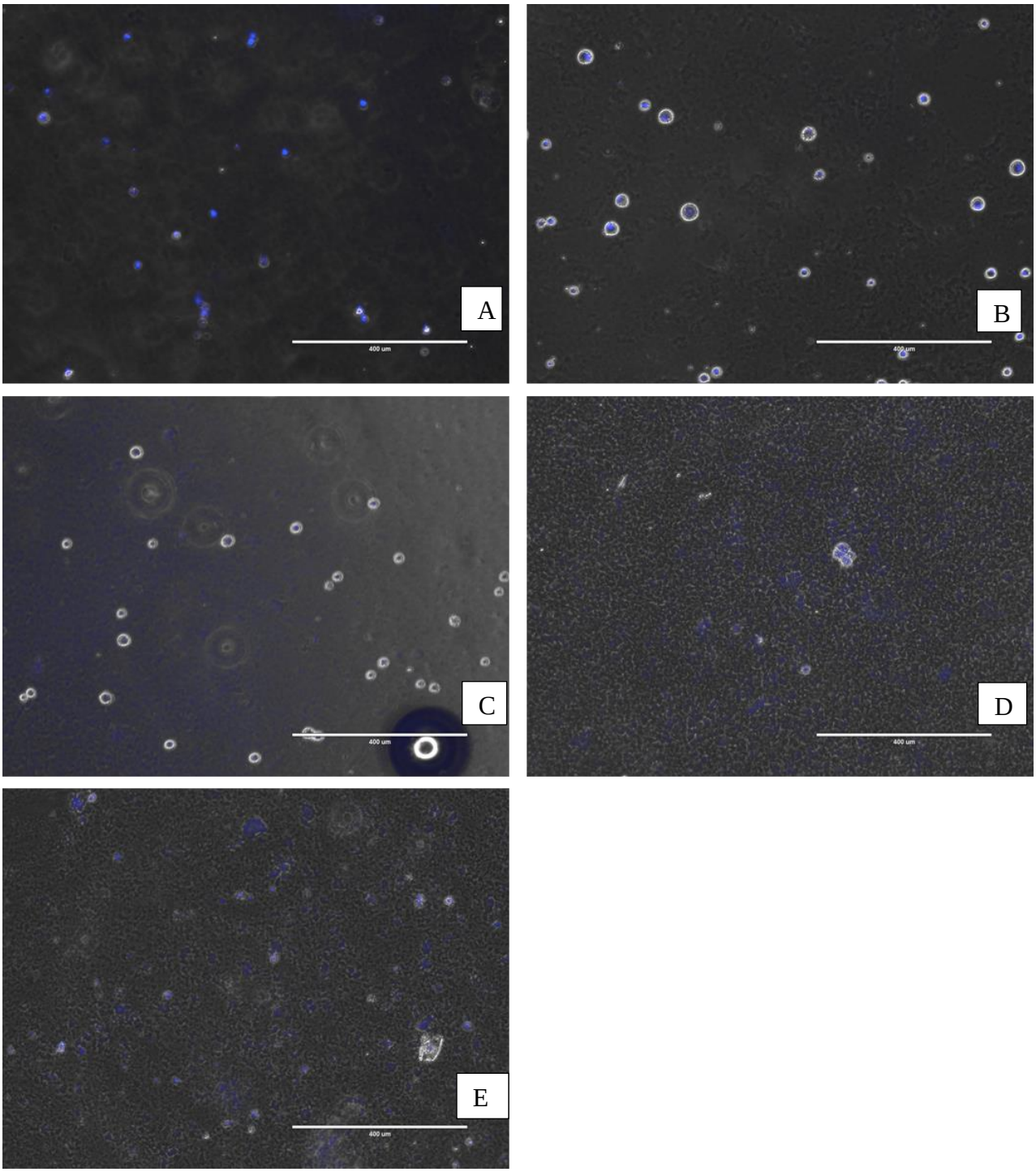

Figure D.8: Cells on 7% BIS crosslinked microgels. A) Unfunctionalized (microgel and cells), functionalized with B) P*+Pep, C) P*+Pep+TGF-B, D) Full Tool, E) Full Tool+TGF-B. All scale bars are 400 microns. Adhesion has improved, but 7% BIS crosslinked microgel samples were by far most difficult to see differences in results between samples in terms of spreading.